

Nuclear activity in galaxy pairs: a spectroscopic analysis of 48 UZC-BGPs. [★]

P., Focardi¹, V. Zitelli², S. Marinoni^{1,3}

¹ Dipartimento di Astronomia, Università di Bologna, Italy
e-mail: paola.focardi@unibo.it

² INAF-OABO, Via Ranzani 1, 40127 Bologna, Italy

³ Fundacion Galileo Galilei & TNG, PO Box 565 S/C de la Palma, Tenerife Spain

Received ; Accepted

ABSTRACT

Context. The role played by interaction on galaxy formation and evolution is a long lasting debated subject. Several questions remain still open, among them if, and to what extent, galaxy interaction may induce nuclear activity

Aims. Galaxy pairs are ideal sites in which to investigate the role of interaction on nuclear activity, for this reason we have undertaken a spectroscopic survey of a large homogeneous sample of galaxy pairs (UZC-BGP)

Methods. We present the results of the nuclear spectral classification, of 48 UZC-BGPs, which represent more than half of the whole sample and have an excellent morphological match with it.

Results. The fraction of emission line galaxies is extremely large, especially among spirals where it reaches 84 % and 95 %, for early and late spirals respectively. SB (Star Burst), is the most frequent type of nuclear activity encountered (30 % of galaxies), while AGNs (Active Galactic Nuclei) are only 19%. The fractions raise to 45 % and 22 % when considering only spirals. Late spirals are characterized by both an unusual increase (35 %) of AGN activity and high luminosity (44 % have $M_B < -20.0 + 5 \log h$). LLAGNs (Low Luminosity AGNs) are only 8% of the total number of galaxies, but this kind of activity could be present in another 10 % of the galaxies (LLAGN candidates). Absorption line galaxies reside mostly (61 %) in S0 galaxies and display the lowest B luminosity in the sample, only 18 % of them have $M_B < -20 + 5 \log h$, but together with LLAGNs (candidates included) they are the most massive galaxies in the sample. Intense-SB nuclei are found in galaxy pairs with galaxy-galaxy projected separations up to $160 h^{-1}$ kpc suggesting that in bright isolated galaxy pairs interaction may be at work and effective up to that distance.

Conclusions. AGNs are characterized by an advanced morphological type while SB phenomenon occurs with the same frequency in early and late spirals. LLAGNs and LLAGN candidates do not always show similar properties, the former are more luminous in B, richer in early-type (E-S0s) galaxies, and half of them are hosted in galaxies showing visible signs of interaction with fainter companions. This last finding suggests that minor interactions might be a driving mechanism for a relevant fraction of LLAGNs. The differences between LLAGNs and LLAGN candidates might confirm, instead, the heterogeneous nature of this class of objects.

Key words. galaxies: general – galaxies: fundamental parameters – galaxies: active – galaxies: interaction

1. Introduction

The role played by interaction on galaxy formation and evolution is a long lasting largely debated subject involving both the “far” and “local” universe. Hierarchical models of galaxy formation invoke, in fact, large occurrence of interaction and merging phenomena, which are expected to increase with redshift (Governato et al. 1999; Gottlober et al. 2001) and affect morphologies, gas distribution and population of galaxies (Dubinski et al. 1996; Mihos & Hernquist 1996). Evolution of the merging rate, with z , has been estimated using close galaxy pairs, but results are, however, conflicting (Zepf & Koo 1989;

Carlberg et al. 1994; Le Fevre et al. 2000; Bundy et al. 2004), which is not unexpected due to differences in sample depths, observational techniques and selection criteria (Patton et al. 2000). Interaction and mergers are less frequent in the “local” universe, but can be analysed with higher detail. Nearby galaxy systems can be investigated at faint luminosity, on a wide spatial scale and with a better knowledge of surrounding environment. However, even “locally” theoretical expectations have not found adequate support from observational data. Galaxy interaction should be, in fact, extremely effective in redistributing large amounts of material towards the galaxy central regions, giving raise, in this way, to violent bursts of star formation (Barnes & Hernquist 1991). Tidal interaction between galaxies is expected to induce instabilities in the discs, able

[★] Based on observations obtained with the Cassini telescope in Loiano (BO)

to generate galaxy bar formations, which, producing an inflow of gas towards the galaxy central regions, may even activate AGN phenomenon (Noguchi 1988; Barnes & Hernquist 1991). However, observations concerning the amount and level of nuclear activity in nearby interacting systems have produced so far conflicting results neither able to confirm, nor to definitely rule out theoretical expectations. In fact, even though, starting with Larson & Tinsley (1978), there has been growing evidence of an increase of star formation in interacting galaxy systems (e.g., Kennicutt & Keel 1984; Kennicutt et al. 1987; Keel 1993, 1996; Donzelli & Pastoriza 1997; Barton et al. 2000), a one-to-one correlation between galaxy-galaxy interaction and star formation remains unclear. Such a correlation holds only for an extremely limited number of objects (ULIRGs, Sanders & Mirabel 1996) which show a fraction of interacting galaxies nearly close to 100 % (Sanders et al. 1988; Borne et al. 1999), while there are several interacting systems with no sign of star formation. The situation becomes even more complex and controversial for the so-called AGN-interaction paradigm for which conflicting results have been given so far (Dahari 1985; Keel et al. 1985; Fuentes-Williams & Stocke 1988; Rafanelli et al. 1995; MacKenty 1989; Kelm et al. 1998; De Robertis et al. 1998; Schmitt 2001; Kelm et al. 2004). However, large part of this contradiction is likely to be ascribed to inhomogeneities among the analyzed samples which are often small, have been selected by different methods and criteria, and may be biased towards or against certain kind of systems.

Galaxy pairs are ideal sites to investigate the role of interaction on nuclear activity since proximity in redshift and in projected separation make interaction and encounters between member galaxies highly probable. The recent availability of a large and complete nearby 3D galaxy catalog (UZC, Falco et al. 1999), has made it feasible to select a volume-limited sample of 89 Bright Galaxy Pairs (UZC-BGPs, Focardi et al. 2006, hereafter paper I) which does not suffer from velocity/distance biases or contamination by projection effects. At variance with previous available nearby pair samples (KPG, Karachentsev et al. 1972, RR Reduzzi & Rampazzo 1989), the first selected visually from the POSS plates, the second applying KPG criteria to the ESO-LV catalog (Lauberts & Valentijn 1989), the UZC-BGP sample has been selected by means of an objective neighbour search algorithm (Focardi & Kelm 2002) applied to the UZC catalog; it is thus complete, homogeneous and contains pairs which are already close in 3D space.

The analysis of UZC-BGP, based on available data (paper I), has allowed us to show that ellipticals are extremely rare and underluminous (in B), while late spirals ($> S_c$) are overluminous. This finding confirms previous claims (Kelm & Focardi 2004) linking the formation of bright ellipticals to group/cluster environment and suggest that galaxy-galaxy interaction might be responsible of the blue luminosity enhancement of disk galaxies through SF phenomena. This last suggestion found support in the strong FIR emission displayed by a significant fraction of early spirals, mostly belonging to interacting pairs.

Very few data are available (see paper I) concerning nuclear activity type in UZC-BGP; we have thus undertaken a spectroscopic survey of the sample. The survey is currently still ongoing

(now 85 % complete). In this paper we present results and analysis for 48 UZC-BGP which constitute more than half of the whole sample and have an excellent morphological match with it.

The sample is presented in (§2); in (§3) we show the results of our nuclear activity classification based on standard diagnostic diagrams; in (§4) we analyze and compare the characteristics of galaxies having different nuclear activity type ; in (§5) we look for possible link of nuclear activity with interaction strength. The conclusions are drawn in §6. In analogy with paper I, a Hubble constant of $H_0 = 100 h \text{ km s}^{-1} \text{ Mpc}^{-1}$ is assumed throughout.

2. The sample

The sample contains 48 galaxy pairs, which represent more than half (54 %) of UZC-BGP sample. The latter is a volume-limited sample of galaxy pairs which has been selected from UZC catalog applying an adapted version of the neighbour search algorithm of Focardi & Kelm (2002). The environment of each UZC galaxy having $M_{Zw} \leq -18.87 + 5 \log h$, $v_r \in [2500-7500] \text{ km s}^{-1}$ and $|b''| \geq 30^\circ$ has been explored on a surrounding area characterized by two projected dimensions ($r_p = 200 h^{-1} \text{ kpc}$ and $R_p = 1 h^{-1} \text{ Mpc}$) and a radial velocity “distance” ($|\Delta v_r| = 1000 \text{ km s}^{-1}$). Galaxies having to only one bright neighbour ($M_{Zw} \leq -18.87 + 5 \log h$) within r_p and $|\Delta v_r|$ and no other ones up to R_p (and within $|\Delta v_r|$) entered the UZC-BGP sample. The adopted value for r_p (galaxy-galaxy projected distance) accounts for possible huge haloes tied to bright galaxies (Bahcall et al. 1995; Zaritsky et al. 1997). The value for $|\Delta v_r|$ is large enough to not induce an artificial cut in the relative velocities of galaxies in pairs (within r_p) and to prevent contamination by galaxy groups/clusters (up to R_p). The value for R_p (large scale isolation radius) was chosen to ensure the absence of luminous companions on group/cluster typical scale. The lower limit in radial velocity was fixed to reduce distance uncertainties due to peculiar motions and to prevent contamination by the Virgo complex, while the upper limit was set to guarantee sampling of UZC luminosity function just below L^* (Cuesta-Bolao & Serna 2003). Finally, the limit in $|b''|$ was imposed to minimize the effects of galactic absorption.

At variance with other galaxy pair samples selected from 3D catalogs (Barton et al. 2000; Alonso et al. 2004), which are magnitude limited and contain pairs belonging to any kind of large scale environment, UZC-BGP is particularly suited to investigate the mutual effect of two bright close companions, isolated on the typical group/cluster scale. Minor companions, which might have failed either UZC ($m_{Zw} \leq 15.5$) or UZC-BGP ($M_{Zw} \leq -18.87 + 5 \log h$) luminosity limit, could be present in the local (within r_p) or distant (within R_p) environment but are not expected to play a role comparable to the one of the two massive galaxies in the pair. UZC-BGP galaxies are, in fact, rather bright and, since luminosity relates to mass although not in an obvious way, rather massive¹ too. (Further details on UZC-BGP sample can be found in paper I).

¹ a rough estimate of the minimum mass (M_{min}) of UZC-BGP galaxies can be derived from their minimum luminosity $L_B \sim 5.5 \cdot 10^9$

Table 1. The E+E pairs

Name	UZC-BGP	Type	T	Emission lines
NGC 2991	23A	S0	-2.1	–
NGC 2994	23B	S0	-2.0	–
NGC 3567	35A	S0	-2.1	–
CGCG 039-055	35B	E	-2.7	–
CGCG 160-030	51A	S0/a	-1.4	–
CGCG 160-036	51B	E	-4.3	[NII] ₆₅₈₃
CGCG 102-023	58A	S0	-1.7	–
CGCG 102-024	58B	S0	-1.8	–
IC 999	63A	S0	-1.9	–
IC 1000	63B	S0	-2.0	–
NGC 6018	77A	SB0/a	-1.2	[NII] ₆₅₄₈ , H α , [NII] ₆₅₈₃ , [SII] ₆₇₁₇ , [SII] ₆₇₃₁
NGC 6021	77B	E	-4.0	[NII] ₆₅₈₃

Following Karachentsev (1972) galaxy pairs can be classified on the basis of their morphological content in E+E, S+S and E+S. E+E contain only early-type galaxies (E + S0s), S+S only spirals and E+S both types. The sample we present here is a fair representation of the whole UZC-BGP as it contains 6 E+E (12 %), 23 S+S (48 %) and 19 E+S (40%), to be compared with 13 %, 48 % and 39 % respectively.

Two dimensional long slit spectra have been acquired with BFOSC (the Bologna Faint Object Spectrograph and Camera) at the 152 cm telescope (of Bologna University) in Loiano. Spectral coverage is 4000-8500 Å with an average resolution of about 4 Å. The slit was positioned on the nucleus of each galaxy and its width was set either at 2'' or at 2.5'', (depending on seeing conditions), which corresponds to galaxy nuclear region (about 500 h^{-1} pc at the average redshift of our sample). The whole data reduction was performed with IRAF. After standard CCD (flat field and bias) correction, we extracted the spectra, calibrated them in wavelength, identified the emission lines and measured their EW. Spectral extraction was limited to the 4-5 central pixels, corresponding to 2''-2.5'' at the detector scale. We set the continuum level in the close neighborhood of each emission line (on both sides) and when the emissions (H α and/or H β) were affected by the presence of an underlying strong absorption line, we set the continuum at the bottom of the emission line, to minimize the effect of the absorption.

Galaxies in E+E, S+S and E+S pairs are listed respectively in Tables 1, 2 and 3. In each Table we give the galaxy name, (column 1), the UZC-BGP identifier (column 2), morphological classification (type) and type code (T) (both from LEDA, columns 3 and 4), emission lines identified in each spectrum, if any, (column 5). We have identified only lines having S/N ≥ 5 , very few lines, however, are characterized by such a low signal, the vast majority has, on average, S/N ≥ 50 . Morphology is very well defined for 86 % (83/96) of the galaxies, less defined for 13 galaxies, in these last cases the morphological classification (column 3) is followed by a question mark.

Inspection of Tables 1 to 3 provides evidence that emission line galaxies are extremely rare in E+E, over abundant

in S+S and rather frequent (more than half of the galaxies) in E+S pairs. In fact, there are 3 galaxies with emission lines in the E+E pairs representing 25 % of the total number of galaxies, 39 emission line galaxies in the S+S (85 %) and 26 in the E+S (68 %) pairs. The different fractions are obviously related to the different morphological content of the pairs and this is clearly illustrated in Fig. 1, whose 4 panels show the morphological distribution of galaxies in the whole sample (upper left), E+E (upper right), S+S (lower left) and E+S (lower right) pairs. Morphology is represented, on the x axis, by means of the type code T (column 4 in each Table), which is a numerical parametrization of the morphological type, introduced by de Vaucouleurs. According to this parametrization, early-type galaxies (E and S0s) have $T < 0$ (E in general $T < -3$), while late spirals ($> \text{Sbc}$) have, on average, $T \geq 4$. The increase of emission line galaxies with morphology is clearly evident in all pair samples containing spiral galaxies (panels 1, 3 and 4 of Fig. 1) and especially in panels 1 and 4 which evidence the larger occurrence of emission features in spiral than in E-S0 galaxies.

The much higher frequency of emission line galaxies among spirals than among early-type (E-S0s) galaxies is not unexpected as emission features occur more frequently in gas rich than in gas poor galaxies; however the two lower panels of Fig.1 show that our sample is characterized by a morphological content which is never more advanced than $T=6$ (corresponding roughly to Sc galaxies). The frequency of emission lines among spirals attains the maximum value for morphologies more advanced than Sc as the the ratio of the current SFR (Star Formation Rate) to the average past one increases from about 0.01 in Sa to 1 in Sc-Irr galaxies (Kennicutt et al. 1994). The large frequency of emission lines occurring among early spirals in our sample might thus be partly induced by interaction.

The two low panels of Fig. 1 show clearly that the fraction of emission galaxies is much lower in E+S than in S+S pairs simply because of the large content of early-type (E-S0s) galaxies in E+S pairs. In fact, in this last sample, 11 of the 12 galaxies with only absorption lines in their spectrum are early-type galaxies, implying that the fractions of early-type galaxies and spirals with emission lines are 42 % (8/19) and 95 % (18/19)

$h^{-2} L_{\odot}$ and assuming, for them, an average M/L of $5 h^{-1}$, this gives $M_{\min} \sim 2.8 \cdot 10^{10} h^{-1} M_{\odot}$.

Table 2. The S+S pairs

Name	UZC-BGP	Type	T	Emission lines
NGC 23	2A	SBa	1.2	[OII] ₃₇₂₇ , H β , [OIII] ₄₉₅₉ , [OIII] ₅₀₀₇ , [OI] ₆₃₀₀ , [NII] ₆₅₄₈ , H α , [NII] ₆₅₈₃ , [SII] ₆₇₁₇ , [SII] ₆₇₃₁
NGC 26	2B	Sab	2.4	[NII] ₆₅₈₃
NGC 800	8A	Sc	5.3	—
NGC 799	8B	SBa	1.1	[NII] ₆₅₄₈ , H α , [NII] ₆₅₄₈ , [SII] ₆₇₁₇ , [SII] ₆₇₃₁
NGC 871	9A	SBc	4.6	[OII] ₃₇₂₇ , H β , [OIII] ₄₉₅₉ , [OIII] ₅₀₀₇ , [OI] ₆₃₀₀ , [NII] ₆₅₄₈ , H α , [NII] ₆₅₈₃ , [SII] ₆₇₁₇ , [SII] ₆₇₃₁ , HeI ₇₀₆₅
NGC 877	9B	SBc	4.8	[NII] ₆₅₄₈ , H α , [NII] ₆₅₈₃ , [SII] ₆₇₁₇ , [SII] ₆₇₃₁
UGC 4074	17A	Sc	5.9	H α
CGCG 262-048	17B	Sc	5.0	[NII] ₆₅₄₈ , H α , [NII] ₆₅₈₃
CGCG 035-023	22A	S?	1.6	H β , [OIII] ₅₀₀₇ , [OI] ₆₃₀₀ , [NII] ₆₅₄₈ , H α , [NII] ₆₅₈₃ , [SII] ₆₇₁₇ , [SII] ₆₇₃₁
CGCG 035-25	22B	S?	2.8	H β , [OIII] ₅₀₀₇ , [NII] ₆₅₄₈ , H α , [NII] ₆₅₈₃ , [SII] ₆₇₁₇ , [SII] ₆₇₃₁
UGC 5241	24A	Sbc	4.4	H β , [OIII] ₄₉₅₉ , [OIII] ₅₀₀₇ , HeI ₅₄₁₂ , [OI] ₆₃₀₀ , H α , [NII] ₆₅₈₃ , [SII] ₆₇₁₇ , [SII] ₆₇₃₁
CGCG 265-043	24B	Sbc	4.3	[NII] ₆₅₄₈ , H α , [NII] ₆₅₈₃
NGC 3303	28A	Sb	3.2	[OII] ₃₇₂₇ , H β , [OIII] ₄₉₅₉ , [OIII] ₅₀₀₇ , [OI] ₆₃₀₀ , [NII] ₆₅₄₈ , H α , [SII] ₆₇₁₇ , [SII] ₆₇₃₁
CGCG 094-098	28B	S?	3.8	[OII] ₃₇₂₇ , H β , [OIII] ₄₉₅₉ , [OIII] ₅₀₀₇ , [OI] ₆₃₀₀ , [NII] ₆₅₄₈ , H α , [NII] ₆₅₈₃ , [SII] ₆₇₁₇ , [SII] ₆₇₃₁
MKN 725	29A	Sc	4.7	H β , [OIII] ₄₉₅₉ , [OIII] ₅₀₀₇ , H α , [NII] ₆₅₈₃ , [SII] ₆₇₁₇ , [SII] ₆₇₃₁ , HeI ₇₀₆₅
UGC 5822	29B	SBa	1.0	[OII] ₃₇₂₇ , H γ , H β , [OIII] ₄₉₅₉ , [OIII] ₅₀₀₇ , HeI ₅₈₇₆ , [OI] ₆₃₀₀ , [NII] ₆₅₄₈ , H α , [NII] ₆₅₈₃ , [SII] ₆₇₁₇ , [SII] ₆₇₃₁
UGC 6033	31A	Sb	3.0	—
CGCG 213-008	31B	S?	0.7	—
UGC 6397	36A	Sab	2.0	[NII] ₆₅₄₈ , H α , [NII] ₆₅₈₃
CGCG 185-053	36B	Sab	1.5	[NII] ₆₅₄₈ , H α , [NII] ₆₅₈₃ , [SII] ₆₇₁₇ , [SII] ₆₇₃₁
NGC 3719	37A	Sbc	3.7	[NII] ₆₅₄₈ , H α , [NII] ₆₅₈₃
NGC 3720	37B	Sa	1.4	H α , [NII] ₆₅₈₃ , [SII] ₆₇₁₇ , [SII] ₆₇₃₁
UGC 7383	44A	Sab	2.0	H β , [OIII] ₅₀₀₇ , H α , [NII] ₆₅₈₃
VCC 0395	44B	Sbc	4.5	[NII] ₆₅₄₈ , H α , [NII] ₆₅₈₃
IC 962	59A	Sa	0.6	[NII] ₆₅₄₈ , H α , [NII] ₆₅₈₃
CGCG 074-014	59B	Sab	1.7	[OIII] ₄₉₅₉ , [OIII] ₅₀₀₇ , [NII] ₆₅₄₈ , H α , [NII] ₆₅₈₃ , [SII] ₆₇₁₇ , [SII] ₆₇₃₁
Mrk 820	66A	S0/a	0.1	[OII] ₃₇₂₇ , H β , [OIII] ₄₉₅₉ , [OIII] ₅₀₀₇ , [NII] ₆₅₄₈ , H α , [NII] ₆₅₈₃ , [SII] ₆₇₁₇ , [SII] ₆₇₃₁
UGC 9464	66B	S0/a	0.0	—
IC 1075	68A	SBb	3.4	[OII] ₃₇₂₇ , H β , [OIII] ₄₉₅₉ , [OIII] ₅₀₀₇ , HeI ₅₈₉₆ , [OI] ₆₃₀₀ , [NII] ₆₅₄₈ , H α , [NII] ₆₅₈₃ , [SII] ₆₇₁₇ , [SII] ₆₇₃₁
IC 1076	68B	Sb	2.8	[NII] ₆₅₄₈ , H α , [NII] ₆₅₈₃ , [SII] ₆₇₁₇ , [SII] ₆₇₃₁
NGC 5797	69A	S0/a	0.0	—
NGC 5804	69B	SBb	3.1	[OII] ₃₇₂₇ , H γ , H β , [OIII] ₄₉₅₉ , [OIII] ₅₀₀₇ , [OI] ₆₃₀₀ , [NII] ₆₅₄₈ , H α , [NII] ₆₅₈₃ , [SII] ₆₇₁₇ , [SII] ₆₇₃₁
NGC 5857	71A	SBab	2.4	[NII] ₆₅₈₃ ,
NGC 5859	71B	SBbc	4.0	[NII] ₆₅₄₈ , H α , [NII] ₆₅₈₃ , [SII] ₆₇₁₇ , [SII] ₆₇₃₁
CGCG 354-023	74A	S?	2.8	[OII] ₃₇₂₇ , H β , [OIII] ₄₉₅₉ , [OIII] ₅₀₀₇ , [OI] ₆₃₀₀ , [NII] ₆₅₄₈ , H α , [NII] ₆₅₈₃ , [SII] ₆₇₁₇ , [SII] ₆₇₃₁
CGCG 354-023	74B	S?	2.8	[OII] ₃₇₂₇ , H β , [OIII] ₄₉₅₉ , [OIII] ₅₀₀₇ , [OI] ₆₃₀₀ , [NII] ₆₅₄₈ , H α , [NII] ₆₅₈₃ , [SII] ₆₇₁₇ , [SII] ₆₇₃₁
IC 4576	76A	S?	0.3	—
IC 4577	76B	S?	1.0	—
NGC 6246	80A	SBb	3.1	H α
NGC 6246 A	80B	SBc	5.1	[NII] ₆₅₄₈ , H α , [NII] ₆₅₈₃ , [SII] ₆₇₁₇ , [SII] ₆₇₃₁
CGCG 452-021	81A	Sc	5.8	H β , [OIII] ₄₉₅₉ , [OIII] ₅₀₀₇ , [NII] ₆₅₄₈ , H α , [NII] ₆₅₈₃ , [SII] ₆₇₁₇ , [SII] ₆₇₃₁
UGC 12067	81B	Sa	1.0	H β , [OIII] ₄₉₅₉ , [OIII] ₅₀₀₇ , [OI] ₆₃₀₀ , [NII] ₆₅₄₈ , H α , [NII] ₆₅₈₃ , [SII] ₆₇₁₇ , [SII] ₆₇₃₁
IC 5242	82A	Sa	1.9	[OII] ₃₇₂₇ , H β , [OIII] ₅₀₀₇ , [NII] ₆₅₄₈ , H α , [NII] ₆₅₈₃ , [SII] ₆₅₈₃ , [SII] ₆₇₃₁
IC 5243	82B	Sbc	3.6	H α
Mrk 308	83A	S0/a	0.3	[OII] ₃₇₂₇ , H γ , H β , [OIII] ₄₉₅₉ , [OIII] ₅₀₀₇ , HeI ₅₈₇₆ , [OI] ₆₃₀₀ , [OI] ₆₃₆₄ , [NII] ₆₅₄₈ , H α , [NII] ₆₅₈₃ , [SII] ₆₇₁₇ , [SII] ₆₇₃₁ , HeI ₇₀₆₅ , [OII] ₇₃₂₅
KUG 2239+200A	83B	Sbc	4.4	[OII] ₃₇₂₇ , H γ , H β , [OIII] ₄₉₅₉ , [OIII] ₅₀₀₇ , HeI ₅₈₇₆ , [OI] ₆₃₀₀ , [NII] ₆₅₄₈ , H α , [NII] ₆₅₈₃ , [SII] ₆₇₁₇ , [SII] ₆₇₃₁ , HeI ₇₀₆₅

respectively. If we compare the last fraction with the fraction (85 %) of emission line galaxies in S+S we see that both E+S and S+S pairs have an equally large probability of hosting an emission line spiral.

Figure 2 shows the absolute magnitude ($M_B - 5 \log h$) distribution of ellipticals ($T < -3$, upper left), S0s ($-3 \leq T < 0$, upper right), early ($0 \leq T < 4$, lower left) and late ($T \geq 4$, lower

right) spirals. (M_B has been derived from B which is available in LEDA, Paturel et al. 2003, for 95/96 galaxies of our sample). In analogy with Fig.1 the continuous distribution refers to the whole samples, the hatched one to galaxies with emission lines. The lower panels of Fig. 2 evidence an extremely large fraction of emission line galaxies in early and late spirals: 84 % (37/44) and 95 % (19/20), respectively. Curiously ellipt-

Table 3. The E+S pairs

Name	UZC-BGP	Type	T	Emission lines
NGC 41	3A	Sc	5.0	[OII] ₃₇₂₇ , [NII] ₆₅₄₈ , H α , [NII] ₆₅₈₃ , [SII] ₆₇₁₇ , [SII] ₆₇₃₁
NGC 42	3B	E/S0	-3.0	–
NGC 160	4A	S0/a	-0.4	–
NGC 169	4B	Sab	2.5	H α , [NII] ₆₅₈₃ , [SII] ₆₇₃₁
NGC 192	5A	SBa	1.0	H β , [OIII] ₄₉₅₉ , [OIII] ₅₀₀₇ , [NII] ₆₅₄₈ , H α , [NII] ₆₅₈₃ , [SII] ₆₇₁₇ , [SII] ₆₇₃₁
NGC 196	5B	SB0	-1.8	–
NGC 997S	10A	E	-3.8	[NII] ₆₅₄₈ , H α , [NII] ₆₅₈₃
NGC 998	10B	S?	2.4	[NII] ₆₅₄₈ , H α , [NII] ₆₅₈₃
Mkn 1076	14A	Sbc	3.8	[OII] ₃₇₂₇ , HeI ₄₀₂₆ , H γ , HeII ₄₆₈₆ , H β , [OIII] ₄₉₅₉ , [OIII] ₅₀₀₇ , [OI] ₆₃₀₀ , [NII] ₆₅₄₈ , H α , [NII] ₆₅₈₃ , [SII] ₆₇₁₇ , [SII] ₆₇₃₁
CGCG 390-059	14B	E/S0	-2.9	–
NGC 1587	16A	E	-4.8	–
NGC 1589	16B	Sab	2.3	[NII] ₆₅₈₃
NGC 2528	18A	SBb	3.1	H γ , H β , [NII] ₆₅₄₈ , H α , [NII] ₆₅₈₃ , [SII] ₆₇₁₇ , [SII] ₆₇₃₁
NGC 2524	18B	S0/a	-0.2	–
NGC 2744	20A	SBab	2.1	[OII] ₃₇₂₇ , HeI ₄₀₂₆ , H δ , H γ , H β , [OIII] ₄₉₅₉ , [OIII] ₅₀₀₇ , HeI ₅₈₇₆ , [OI] ₆₃₀₀ , [NII] ₆₅₄₈ , H α , [NII] ₆₅₈₃ , [SII] ₆₇₁₇ , [SII] ₆₇₃₁
NGC 2749	20B	E	-4.8	[NII] ₆₅₄₈ , H α , [NII] ₆₅₈₃ , [SII] ₆₇₁₇ , [SII] ₆₇₃₁
NGC 2872	21A	E	-4.8	–
NGC 2874	21B	SBbc	4.4	[NII] ₆₅₄₈ , H α , [NII] ₆₅₈₃ , [SII] ₆₇₁₇ , [SII] ₆₇₃₁
CGCG 008-034	26A	Sb	2.5	[NII] ₆₅₈₃
IC 590 N	26B	E/S0	-3.2	H α , [NII] ₆₅₈₃
CGCG 065-023	27A	S0/a	-1.0	[NII] ₆₅₄₈ , H α , [NII] ₆₅₈₃
UGC 5627	27B	Sab	1.7	[NII] ₆₅₄₈ , H α , [NII] ₆₅₈₃
NGC 4003	39A	SB0	-1.9	H α , [NII] ₆₅₈₃
NGC 4002	39B	Sa	1.4	[NII] ₆₅₈₃
NGC 4446	49A	Sc	5.8	H β , [OI] ₆₃₀₀ , [NII] ₆₅₄₈ , H α , [NII] ₆₅₈₃
NGC 4447	49B	SB0	-2.2	–
CGCG162-059	61A	SBbc	4.4	[NII] ₆₅₄₈ , H α , [NII] ₆₅₈₃
UGC 9012	61B	S0	-2.0	–
UGC 9413	65A	Sbc	4.0	[OII] ₃₇₂₇ , H β , [OIII] ₄₉₅₉ , [OIII] ₅₀₀₇ , [NII] ₆₅₄₈ , H α , [NII] ₆₅₈₃ , HeI ₆₆₇₈ , [SII] ₆₇₁₇ , [SII] ₆₇₃₁
CGCG 353-044	65B	S0	-1.7	–
NGC 5771	67A	E	-4.5	–
NGC 5773	67B	Sa	1.4	–
CGCG 136-013	75A	E?	-0.8	[NII] ₆₅₈₃
CGCG 136-015	75B	S?	2.2	[NII] ₆₅₄₈ , H α , [NII] ₆₅₈₃
NGC 6251	79A	E	-4.8	[OIII] ₅₀₀₇ , [NII] ₆₅₄₈ , H α , [NII] ₆₅₈₃
NGC 6252	79B	S?	4.4	[NII] ₆₅₈₃
IC 5285	84A	E?	-0.8	[NII] ₆₅₈₃
NGC 7489	84B	Sc	6.5	H α , [NII] ₆₅₈₃

ticals (upper left) also show an unusually large content (67 %) of emission line galaxies, but the statistics are too poor and do not allow us to draw definitive conclusions on this point. S0 galaxies, instead, are quite abundant in our sample (22/96) and appear to host a much more limited fraction (23 %) of emission line galaxies. From Fig. 2 we see that our sample is numerically dominated by early spirals (47 %), has an almost equal content of late spirals (21 %) and S0s (23 %) and contains a limited fraction (9 %) of ellipticals. In terms of luminosity (M_B) S0s are characterized by a larger content of "faint" galaxies, about half of them (12/22, 55 %) have $M_B \geq -19.5 + 5 \log h$. There are no ellipticals with M_B larger than that value, while early and late spirals (with $M_B \geq -19.5 + 5 \log h$) represent, respectively, 25 % and 15 % of each whole population. Further investigation is required to establish whether the population of

low luminosity S0s is typical of bright galaxy pairs and if the lack of emission features in these galaxies relates to their low luminosity either.

Figure 3 shows the distribution of galaxy-galaxy projected distance (r_p , upper panels) and velocity separation ($|\Delta v_r|$, lower panels) for E+E, S+S and E+S pairs. The continuous distribution indicates the whole samples, the dashed distributions indicate pairs having at least one member with emission line spectrum (double dash) and pairs in which both members have emission lines (single dash). The fraction of pairs having both members "active" is clearly larger in S+S (78 %, 18/23) than in E+S (42 %, 8/19). This difference is induced by the early-type galaxy content of the E+S pairs. The fractions become, in fact, similar (91 % and 95 %) when considering S+S and E+S pairs in which at least one member has an emission line spectrum.

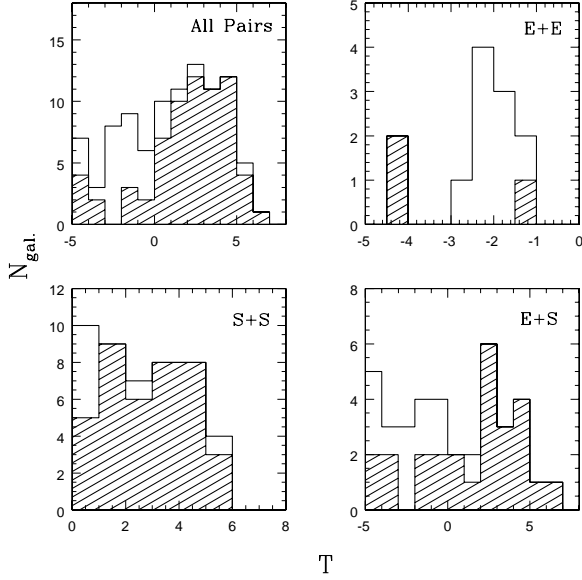


Fig. 1. Relation between pair morphology and the presence of emission lines in the member galaxy spectra. Continuous histogram show the morphological distribution of the whole galaxy pair sample (upper left), of E+E (upper right), S+S (lower left) and E+S (lower right) pairs. Dashed histograms indicate morphological distribution of galaxies with emission line spectrum, in each sample.

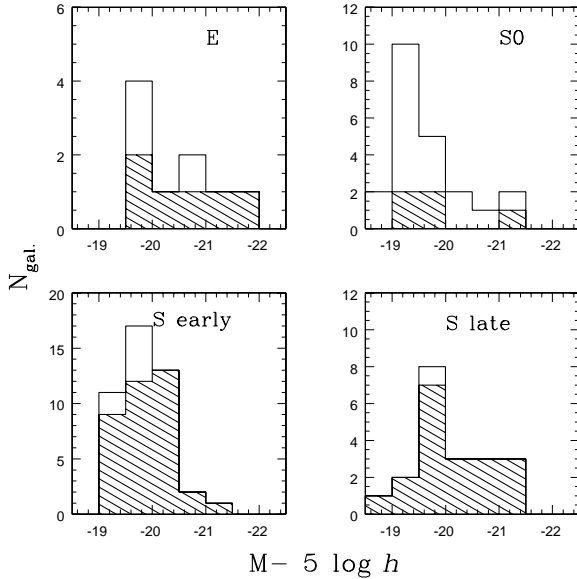


Fig. 2. Absolute magnitude (M_B) distribution of galaxies, of different morphological types, having or not having emission lines in their spectra. Continuous distribution refer to the whole samples, hatched one to galaxies with emission lines.

Previous work (Barton et al. 2000; Alonso et al. 2004) has claimed an increase of emission line galaxies in pairs with decreasing member projected distances. In our sample the fraction of emission line galaxies in E+S and S+S pairs is so high, at all member distances, that we hardly see such an effect. We

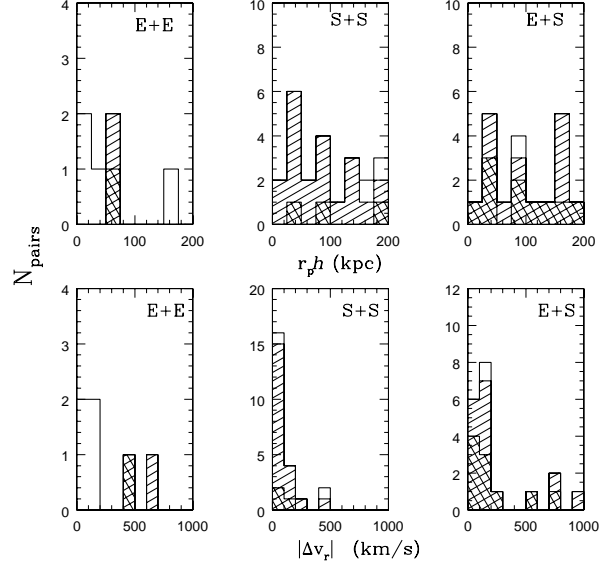


Fig. 3. Relation between the presence of emission lines in the galaxy spectra and dynamical parameters of the pairs. The upper panels show the galaxy-galaxy projected distance (r_p) distribution, the lower panels the velocity difference ($|\Delta v_r|$) between galaxies (in each pair) for E+E, S+S, E+S respectively. Pairs having at least one galaxy with emission spectrum are represented by dashed histogram. The single dash indicates pairs in which both members have an emission line spectrum, the double dash pairs hosting only one emission line galaxy.

stress however that UZC-BGP is a volume limited sample of bright isolated galaxy pairs quite different from magnitude limited samples of close pairs belonging to any kind of environment as are the samples on which Barton et al. (2000) and Alonso et al. (2004) evidenced the distance effect. The very large fraction of emission line galaxies in our sample at all pair distances may actually indicate that in isolated pairs of luminous ($M_{Zw} \leq -18.9 + 5 \log h$) galaxies interaction is at work and effective up to $200 h^{-1}$ kpc. Both Barton et al. (2000) and Alonso et al. (2004) find the emission line enhancement on a much smaller scale ($\sim 30 h^{-1}$ kpc). Their result is likely to indicate that when galaxy pairs are surrounded by companions of comparable luminosity galaxy-galaxy interaction becomes effective only at very small distances. Our result indicates that fainter companions which may be present in some UZC-BGP systems in the close ($200 h^{-1}$ kpc and/or large ($1 h^{-1}$ Mpc surrounding area do not play an action comparable to the one of luminous member galaxies.

The lower panels of Fig. 3 indicate a “dynamical” difference between pairs containing only spirals (middle panel) and pairs containing either both (left panel) or at least one (right panel) early-type galaxy, the former being characterized by a narrower $|\Delta v_r|$ distribution than the latter ones (KS confidence level 93.9 % and 99.9 % respectively). This difference (already outlined in paper I) suggests that E+S and E+E pairs might actually be embedded within large loose structures as their broader $|\Delta v_r|$ distribution would indicate the presence of

a larger potential well. In this framework the emission spectrum of the 3 early-type galaxies belonging to the E+E pairs could arise from infalling of these galaxies within a loose group as suggested from their large $|\Delta v_r|$ value. We have checked this hypothesis and found that neither UZC-BGP 51 nor UZC-BGP 77 are part of any known galaxy group. However, inspection of available (LEDA) redshifts of galaxies in the surrounding environment of both pairs show that UZC-BGP 51 might be part of a loose galaxy group which could possibly be infalling on the nearby ($4 h^{-1}$ Mpc) Coma cluster; while UZC-BGP 77A (NGC 6018) might be infalling on a galaxy loose group having the same radial velocity of UZC-BGP 77B (NGC 6021). More investigation is required to confirm our hypothesis.

3. Nuclear activity classification

To classify nuclear activity in our galaxy sample, we have made use of the standard diagnostic diagrams (Baldwin et al. 1981; Veilleux & Osterbrock 1987; Veilleux 2002), also known as the BPT diagrams, which have proved to be an extremely efficient method to distinguish the different types of activity encountered in emission line galaxies (Veilleux et al. 1995; Veron et al. 1997; Gonçalves et al. 1999). Moreover, being based on ratios of emission lines which are very close in wavelength they are almost unaffected by reddening corrections (Veilleux & Osterbrock 1987). The diagnostic diagrams relate $[\text{OIII}]_{5007}/\text{H}_\beta$ to $[\text{NII}]_{6583}/\text{H}_\alpha$, $[\text{SII}]_{(6717+6731)}/\text{H}_\alpha$ and $[\text{OI}]_{6300}/\text{H}_\alpha$.

Of the 68 galaxies with emission spectra (cfr. Tables 1,2 and 3), 24 allowed us to build up from one to three of the above mentioned standard diagnostic diagrams. These galaxies are listed in Table 4, in order of decreasing number of diagnostic diagrams, i.e. the first 14 galaxies have all line ratios measured, the subsequent 8 galaxies only three line ratios and the remaining 2 only two. Table 4, reports, for these galaxies, UZC-BGP identifier (column 1), pair/galaxy morphology (column 2, galaxy morphology is underlined in cases of mixed pair morphology), line ratios and errors (column 3,4,5,6). Each line ratio has been obtained averaging line ratios obtained independently by each of us and the associated error represent the standard deviation (σ). The vast majority (20/24) of galaxies listed in Table 4 belongs to the S+S pair sample and the remaining 4 are however spirals, implying that there are no early-type galaxies in our sample showing at least 4 emission lines.

The $\text{Log}([\text{OIII}]_{5007}/\text{H}_\beta)$ versus $\text{Log}([\text{NII}]_{6583}/\text{H}_\alpha)$ diagram (hereafter diag. 1), for all the galaxies listed in Table 4, is shown in Fig. 4. Different symbols indicate different nuclear activity according to Veilleux & Osterbrock (1987) empirical classification (hereafter VO87) which separates high from low excitation galaxies (Seyfert 2 from LINERs and HII galaxies from SBs) based on a $[\text{OIII}]_{5007}/\text{H}_\beta$ value of 3 and LINER from SBs based on a $[\text{NII}]_{6583}/\text{H}_\alpha$ value of 0.6.

According to VO87, our sample contains one Seyfert 2 galaxy (triangle), two LINERs (squares) and 21 SBs (circles). The Sy 2 (UZC-BGP 83A) and the LINERs (UZC-BGP 28A and 69B) are identified in Fig. 4. On the same diagram we show two curves, the solid one to the left is the Kauffman et al. (2003) sequence (hereafter Kauff03), the dotted one to the right is the Kewley et al. (2001) sequence (hereafter Kew01). Both se-

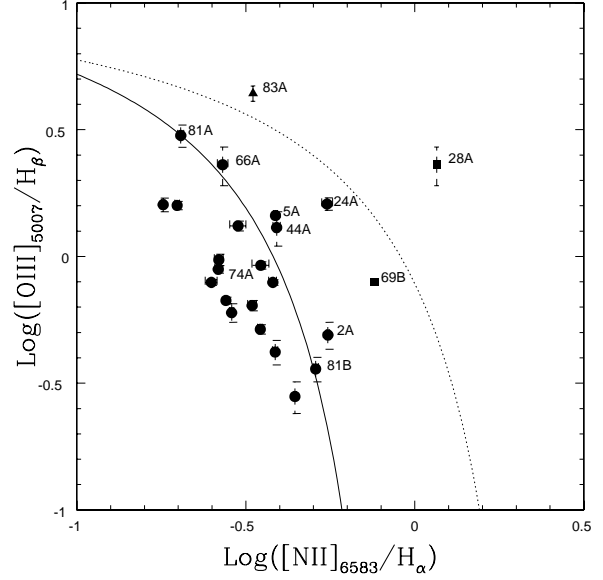


Fig. 4. $\text{Log}([\text{OIII}]_{5007}/\text{H}_\beta)$ versus $\text{Log}([\text{NII}]_{6583}/\text{H}_\alpha)$ diagnostic diagram (diag. 1). Circles, squares and triangle indicate classification into SB, LINER and Sy 2 according to VO87 scheme. The solid curve on the left is the Kauff03 sequence, while the dotted curve on the right corresponds to the Kew01 sequence. Both sequences are supposed to separate SB from AGNs. Identification is provided for all galaxies above Kauff03 sequence as, according to it, they should all be classified as AGNs. One galaxy (UZC-BGP 74A) below the Kauff03 sequence has been identified too as it lays in the LINER region of diag. 3.

quences are supposed to separate SB from AGNs. Kauff03 is an empirical sequence which has been derived from a huge sample ($\sim 22\,000$) of SDSS emission line galaxies, while Kew01 is a theoretical sequence derived using a wide set of models accounting for photoionization and stellar population synthesis. Figure 4 shows that there are 8 galaxies falling between Kauff03 and Kew01 sequences. These galaxies, ordered by decreasing value of $[\text{OIII}]_{5007}/\text{H}_\beta$, are UZC-BGP 81A, 66A, 24A, 5A, 44A, 69B (a LINER according to VO87), 2A and 81B and have all been identified in Fig. 4. Two of these galaxies (UZC-BGP 81A and 66A) could fall just below the Kauff03 sequence taking into account the error associated to the $[\text{OIII}]_{5007}/\text{H}_\beta$ measure, while another one (UZC-BGP 81B) would move from just above the sequence to the sequence itself. One further galaxy (UZC-BGP 74A) is identified in Fig. 4 as although it lays, in this diagram, well below the Kauff03 sequence, it occupies the LINER region of diag. 3 (Fig. 6)

Figure 5 shows the $\text{Log}([\text{OIII}]_{5007}/\text{H}_\beta)$ versus $\text{Log}([\text{SII}]_{(6717+6731)}/\text{H}_\alpha)$ diagram (hereafter diag. 2) for the 22 galaxies of Table 4 which have also these line ratios measured. In analogy with Fig. 4 different symbols stand for different classification in the VO87 scheme ($[\text{OIII}]_{5007}/\text{H}_\beta \geq 3$ and $[\text{SII}]_{(6717+6731)}/\text{H}_\alpha \geq 0.4$ separate, respectively, Sy 2 and LINER from SBs). VO87 criteria confirm the classification in Sy 2 and LINERs obtained from diag. 1 (Fig. 4) for UZC 83A,

Table 4. Spectral line ratios for standard diagnostic diagrams (diags. 1, 2 and 3).

UZC-BGP	Pair type	[OIII] ₅₀₀₇ /H β	[NII] ₆₅₈₃ /H α	[SII] ₍₆₇₁₇₊₆₇₃₁₎ /H α	[OI] ₆₃₀₀ /H α
2A	S+S	0.49 \pm 0.06	0.553 \pm 0.006	0.333 \pm 0.004	0.043 \pm 0.002
9A	S+S	1.59 \pm 0.06	0.198 \pm 0.003	0.382 \pm 0.006	0.035 \pm 0.006
14A	E+S	0.516 \pm 0.022	0.349 \pm 0.006	0.278 \pm 0.023	0.022 \pm 0.008
20A	E+S	1.32 \pm 0.06	0.30 \pm 0.01	0.36 \pm 0.02	0.023 \pm 0.002
24A	S+S	1.61 \pm 0.09	0.55 \pm 0.02	0.25 \pm 0.03	0.045 \pm 0.000
28A	S+S	2.3 \pm 0.4	1.16 \pm 0.02	0.70 \pm 0.05	0.40 \pm 0.04
28B	S+S	0.67 \pm 0.02	0.276 \pm 0.002	0.19 \pm 0.01	0.023 \pm 0.006
29B	S+S	0.60 \pm 0.05	0.287 \pm 0.004	0.20 \pm 0.01	0.021 \pm 0.003
68A	S+S	0.79 \pm 0.02	0.25 \pm 0.01	0.21 \pm 0.02	0.044 \pm 0.007
74A	S+S	0.92 \pm 0.03	0.35 \pm 0.02	0.22 \pm 0.01	0.54 \pm 0.03
74B	S+S	1.6 \pm 0.1	0.18 \pm 0.02	0.232 \pm 0.003	0.05 \pm 0.01
81B	S+S	0.36 \pm 0.04	0.509 \pm 0.009	0.17 \pm 0.02	0.028 \pm 0.003
83A	S+S	4.4 \pm 0.3	0.332 \pm 0.003	0.144 \pm 0.006	0.078 \pm 0.005
83B	S+S	0.89 \pm 0.03	0.262 \pm 0.006	0.26 \pm 0.01	0.044 \pm 0.003
5A	E+S	1.45 \pm 0.02	0.387 \pm 0.005	0.248 \pm 0.005	-
22A	S+S	0.79 \pm 0.02	0.38 \pm 0.01	0.17 \pm 0.01	-
22B	S+S	0.64 \pm 0.03	0.33 \pm 0.01	0.28 \pm 0.02	-
29A	S+S	0.28 \pm 0.04	0.442 \pm 0.004	0.102 \pm 0.008	-
66A	S+S	2.3 \pm 0.4	0.27 \pm 0.01	0.198 \pm 0.004	-
69B	S+S	0.79 \pm 0.02	0.76 \pm 0.02	0.51 \pm 0.03	-
81A	S+S	3.0 \pm 0.3	0.203 \pm 0.004	0.18 \pm 0.02	-
82A	S+S	0.42 \pm 0.04	0.386 \pm 0.004	0.18 \pm 0.02	-
44A	S+S	1.3 \pm 0.2	0.39 \pm 0.01	-	-
65A	E+S	0.97 \pm 0.05	0.263 \pm 0.008	-	-

28A and 69B. The dotted curve and line correspond to Kew01 and Kew06 (Kewley et al. 2006) sequences. The former one separates SB (below) from AGNs (above), the latter one Sy 2 (above) from LINERs (below). Identified, on this plot, are also the three confirmed (VO87) AGNs and 7 (of the 8) galaxies laying between Kauff03 and Kew01 sequences in diag. 1 (Fig. 4), as UZC-BGP 44A has only diag. 1 available (cfr. Table 4). Finally the position of UZC-BGP 74A is indicated, since this galaxy occupies the LINER region of diag. 3 (Fig. 6).

Figure 5 shows that, according to Kew01 and Kew06 classification, only one galaxy (UZC-BGP 28A) would be classified as LINERs. All the others would be SB, although UZC-BGP 83A (Sy 2 following VO87 scheme) lies just below the Kew01 sequence and would move exactly on it if one lets [OIII]₅₀₀₇/H β attain its maximum possible value (within the error).

Figure 6 shows the Log ([OIII]₅₀₀₇/H β) versus Log ([OI]₆₃₀₀/H α) diagram (hereafter diag. 3) for the 14 galaxies in Table 4 having these line ratios measured. In analogy with Figs. 4 and 5 different symbols represent different nuclear activity types according to VO87 scheme which separates Sy 2 from SB and LINERs based on a value of [OIII]₅₀₀₇/H β of 3 and requires a value of [OI]₆₃₀₀/H α \geq 0.08 for Sy 2 and \geq 0.17 for LINERs. Here too the dotted curve and line correspond to Kew01 and Kew06 sequences separating SB from AGNs and Sy 2 from LINERs respectively. Identified, in this plot, are all the galaxies lying above Kew01 curve and 3 (over 8) galaxies lying in the Kauff03 Kew01 region of diag. 1 (Fig. 4). Two galaxies (UZC-BGP 28A and 74A) occupy the Kew01 – Kew06 LINER region, one (UZC-BGP 83A) the Sy 2 region. This classification is confirmed by VO87. One galaxy in Fig. 6 (UZC-BGP

74B) could move from the SB locus to the Kew01 SB/AGN separation curve when taking into account the error associated to the [OI]₆₃₀₀/H α measure. This galaxy is very close to UZC-BGP 24A (at its right), but we have not identified it in Fig. 6, as it occupies the SB region both in diags. 1 and 2.

The spectral analysis of the 24 emission line galaxies listed in Table 4 allow us to classify unambiguously 14 of them as for these galaxies all the different classification schemes (VO87, Kauff03 and Kew01-06) give consistent results on the 3 diagnostic diagrams. Of the remaining 10 galaxies 8 lay above the Kauff03 sequence and below the Kew01 in diag. 1. One (UZC-BGP 44A), of these 8, has only diag. 1 available, 4 have also diag. 2 and 3 have both diags. 2 and 3 available. VO87 and Kew01 classification schemes agree on SB activity in the other diagnostic diagrams for 6 of the 7 galaxies having either both diag. 2 and diag. 3 or only diag. 2 available, only UZC-BGP 69B is classified (in diag. 2) LINER in the VO87 scheme and SB in the Kew01 one. The 2 other “difficult” cases are UZC-BGP 83A and 74A. The first one is a Sy 2 in both diags. 1 and 3, for all classification schemes, but in diag. 2 is a SB, according to Kew01 (although it lays very close to the SB/AGN border and would sit exactly on it if [OIII]₅₀₀₇/H β attains its maximum permitted value within the error), and a Sy 2 according to VO87. More “difficult” is the case of UZC-BGP 74A which is a LINER in diag. 3 (for both Kew01 and VO87) and a SB in diags. 1 and 2 for all classification schemes.

Galaxies displaying different kind of nuclear activity, in different diagnostic diagrams, should be classified as composite objects (Kewley et al. 2006). However, in order to avoid double classification (e.g. SB/AGN, Sy2/SB, LINER/SB) we have

Table 5. Spectral line ratios for diag. 4

UZC-BGP	Pair type	$[\text{NII}]_{6583}/\text{H}_\alpha$	$[\text{NII}]_{6583}$
3A	E+S	0.45 ± 0.01	5.1 ± 0.8
4B	E+S	2.99 ± 0.01	1.01 ± 0.01
8B	S+S	0.34 ± 0.02	4.2 ± 0.3
9B	S+S	0.332 ± 0.004	3.71 ± 0.06
10A	<u>E</u> +S	1.27 ± 0.08	2.11 ± 0.04
10B	E+S	0.85 ± 0.02	2.9 ± 0.1
17B	S+S	0.337 ± 0.004	5.97 ± 0.04
18A	E+S	0.245 ± 0.007	12.0 ± 0.4
20B	<u>E</u> +S	2.9 ± 0.1	2.9 ± 0.1
21B	E+S	9.4 ± 1.6	2.8 ± 0.2
24B	S+S	0.61 ± 0.02	6.4 ± 0.3
26B	<u>E</u> +S	2.8 ± 0.8	1.3 ± 0.3
27A	<u>E</u> +S	3.0 ± 0.4	4.76 ± 0.07
27B	E+S	0.50 ± 0.04	4.4 ± 0.2
36A	S+S	2.5 ± 0.4	3.5 ± 0.6
36B	S+S	0.58 ± 0.02	5.8 ± 0.2
37A	S+S	0.70 ± 0.03	3.6 ± 0.3
37B	S+S	0.36 ± 0.02	5.5 ± 0.5
39A	<u>E</u> +S	0.838 ± 0.006	6.4 ± 0.1
44B	S+S	0.57 ± 0.02	6.2 ± 0.2
49A	E+S	0.375 ± 0.005	7.7 ± 0.3
59B	S+S	0.650 ± 0.008	6.10 ± 0.07
61A	E+S	0.752 ± 0.07	7.8 ± 0.3
68B	S+S	0.36 ± 0.01	4.0 ± 0.3
71B	S+S	3.2 ± 0.1	3.8 ± 0.2
75A	<u>E</u> +S	1.565 ± 0.007	2.55 ± 0.07
75B	E+S	0.95 ± 0.01	2.7 ± 0.3
77A	E+E	0.74 ± 0.03	4.5 ± 0.3
79A	<u>E</u> +S	1.65 ± 0.06	4.4 ± 0.4
80B	S+S	0.28 ± 0.06	8.1 ± 0.3
84B	E+S	0.44 ± 0.02	4.42 ± 0.02

decided to assign to each galaxy the "most frequent" classification according to different schemes applied to the 3 diagnostic diagrams. We keep, however, record of each classification scheme in each diagnostic diagram in Table 6, which summarizes the results of our spectral analysis.

A large fraction of emission line galaxies (31/68) have well defined H_α and $[\text{NII}]$ lines but do not show $[\text{OIII}]$ and/or H_β features and thus does not allow us to use the standard diagnostic diagrams. For these galaxies, listed in Table 5, the activity type can be classified (Coziol et al. 1998) comparing the EW of $[\text{NII}]_{6583}$ feature with the ratio of $[\text{NII}]_{6583}$ to H_α . These values are listed in Table 5, together with their errors, which, in analogy with Table 4, represent respectively the average of 3 measures obtained independently by each of us and the associated σ . The underlined morphology in column 2 indicates, as in Table 4, the "rough" galaxy morphology when galaxy pair is of mixed (E+S) type.

Following Coziol et al. (1998) we have classified the 31 galaxies listed in Table 5 as SB if they have $\text{Log}([\text{NII}]_{6583}/\text{H}_\alpha) < -0.4$ and $\text{Log EW}([\text{NII}]_{6583}) \geq 0.5$; AGN and LLAGN if they have $\text{Log EW}([\text{NII}]_{6583}/\text{H}_\alpha) \geq -0.4$ and $\text{Log EW}([\text{NII}]_{6583}) \geq 0.5$ or < 0.5 respectively. The lines which separate the loci of SB, AGN and LLAGN are represented in Fig. 7 which

shows the $\text{Log EW}([\text{NII}]_{6583})$ versus $\text{Log}([\text{NII}]_{6583}/\text{H}_\alpha)$ diagram (hereafter diag. 4) for the 31 galaxies listed in Table 5 (filled circles). Among these galaxies we have identified the ones (7), showing the largest value of $[\text{NII}]_{6583}/\text{H}_\alpha$. This behaviour is due to the presence of a strong H_α feature in absorption depressing the emission one and resulting in an enhanced $[\text{NII}]_{6583}/\text{H}_\alpha$ ratio. From Fig. 7 we see that only one galaxy (UZC-BGP 36A) could have its classification changed (from AGN to LLAGN) when taking into account the error associated to $\text{EW}([\text{NII}]_{6583})$ measure.

The classification scheme adopted by Coziol et al. (1998) is empirical and might, thus, be questioned, for this reason we also show, on the same plot (Fig. 7), the 24 galaxies (open symbols) listed in Table 4, that we have classified by means of one or more standard diagnostic diagrams. The different symbols indicate (in analogy to Figs. 4, 5, and 6) different nuclear activity kind. From Fig. 7 we see that for low values of $\text{Log EW}([\text{NII}]_{6583})$ ($\sim < 1.1$) Coziol classification scheme holds well, since all galaxies classified as SB (open circles) occupy the SB region of the diagram, whereas for larger values of $\text{Log EW}([\text{NII}]_{6583})$ there are SBs in the AGN region and AGN in the

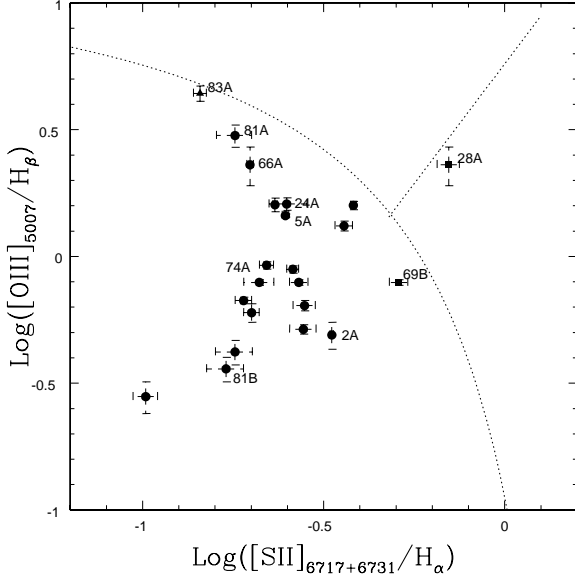


Fig. 5. $\text{Log} ([\text{OIII}]_{5007}/\text{H}\beta)$ versus $\text{Log} ([\text{SII}]_{6717+6731}/\text{H}\alpha)$ diagnostic diagram (diag. 2). In analogy with Fig. 4, circles, squares and triangle indicate classification into SB, LINER and Sy 2 according to VO87 scheme. The dotted curve represent the Kew01 sequence separating SB (below) from AGN (above) region. The dotted line is the Kew06 sequence which separate Seyfert (above) from LINERs (below). Identified on this plot are all the galaxies above the Kauff03 sequence in diag.1 and UZC-BGP 74A.

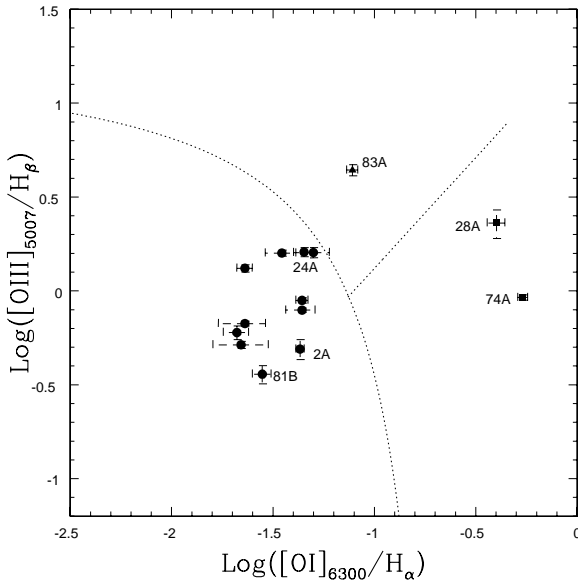


Fig. 6. $\text{Log} ([\text{OIII}]_{5007}/\text{H}\beta)$ versus $\text{Log} ([\text{OI}]_{6300}/\text{H}\alpha)$ diagnostic diagram (diag. 3). Symbols are as in Fig. 4 and 5. In analogy with Fig. 5 the dotted curve and line represent Kew01 and Kew06 sequences separating, respectively, SB from AGNs and Seyfert from LINERs. Identification is provided for all the galaxies lying in the “AGN” region either in this or in another diagnostic diagram.

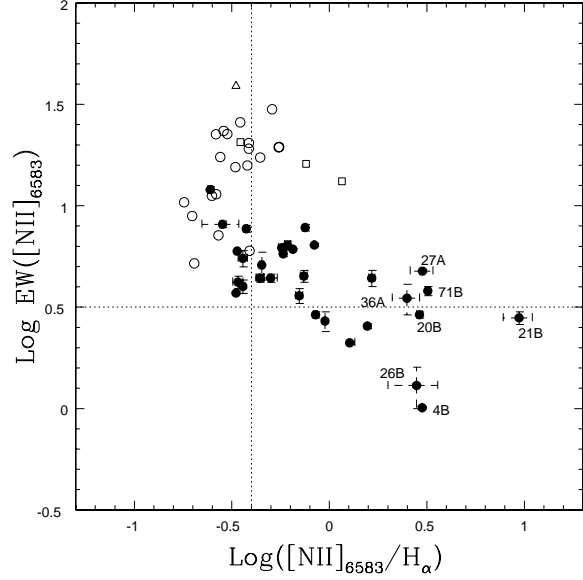


Fig. 7. $\text{Log EW} ([\text{NII}]_{6583})$ versus $\text{Log} ([\text{NII}]_{6583}/\text{H}\alpha)$ diagnostic diagram (diag. 4) that we have used to classify the 31 galaxies listed in Table 5 (filled circles). The vertical dotted line separates the SB locus from the AGN one, the horizontal dotted line separates AGNs (up) from LLAGNs (low). The open symbols indicate the position, in this diagram, of the 24 galaxies listed in Table 4, whose nuclear activity has been classified by means of one or more standard diagnostic diagrams. (Circles, squares and triangle indicate classification into SB, LINER and Sy 2 according to VO87 scheme applied to diags. 1, 2 and 3).

SB ones². The agreement between Coziol and standard classification, occurring at low values of $\text{Log EW} ([\text{NII}]_{6583})$, where SBs from Tables 4 and 5 overlap, make us to feel rather confident about this classification scheme.

Of the remaining 13 galaxies with emission lines (cfr. Tables 1, 2 and 3), 10 show only the $[\text{NII}]_{6583}$ emission feature and thus, according to Coziol et al. (1998) we have classified them as LLAGN candidates, while 3 show only $\text{H}\alpha$ in emission and have not been classified.

Table 6 summarizes the nuclear activity classification for 65/68 emission line galaxies of our sample. The classification has been performed on the basis of one, or more, diagnostic diagrams for 55 galaxies and on the presence of the unique emission feature $[\text{NII}]_{6583}$, for 10, that following Coziol et al. (1998) we have classified as LLAGN candidates. Three galaxies (UZC-BGP 17A, 80A and 82B) show only $\text{H}\alpha$ in emission and thus could not be classified and included in Table 6. Besides UZC-BGP identifier (column 1) and pair/galaxy morphology (column 2, as in Tables 4 and 5 galaxy morphology is underlined in E+S pairs), Table 6 lists the classification derived from diags. 1, 2 and 3 (columns 3, 4 and 5), according to VO87 (first subcolumn), Kew01 (second subcolumn) and Kauff03 (third subcolumn, only for diag. 1). In column 6 the

² This behaviour is not unexpected since the sequence which separates AGN from SBs, in Fig. 4, is bended in $[\text{NII}]_{6583}/\text{H}\alpha$ and Sy 2 are characterized by lower values of $[\text{NII}]_{6583}/\text{H}\alpha$ than LINERs.

UZC-BGP	Pair type	Diag. 1			Diag. 2		Diag. 3		Diag. 4	Adopted	Known
		VO87	Kew01	Kauff03	VO87	Kew01	VO87	Kew01			
2A	S+S	SB	SB	AGN	SB	SB	SB	SB		SB	SB
2B	S+S	—	—	—	—	—	—	—		LL:	
3A	E+S	—	—	—	—	—	—	—	AGN	AGN	LINER
4B	E+S	—	—	—	—	—	—	—	LLAGN	LLAGN	
5A	E+S	SB	SB	AGN	SB	SB	—	—		SB	HII
8B	S+S	—	—	—	—	—	—	—	SB	SB	
9A	S+S	SB	SB	SB	SB	SB	SB	SB		SB	
9B	S+S	—	—	—	—	—	—	—	SB	SB	
10A	E+S	—	—	—	—	—	—	—	LLAGN	LLAGN	
10B	E+S	—	—	—	—	—	—	—	LLAGN	LLAGN	
14A	E+S	SB	SB	SB	SB	SB	SB	SB		SB	SB
16B	E+S	—	—	—	—	—	—	—		LL:	
17B	S+S	—	—	—	—	—	—	—	SB	SB	
18A	E+S	—	—	—	—	—	—	—	SB	SB	LLIRG
20A	E+S	SB	SB	SB	SB	SB	SB	SB		SB	
20B	E+S	—	—	—	—	—	—	—	LLAGN	LLAGN	
21B	E+S	—	—	—	—	—	—	—	LLAGN	LLAGN	
22A	S+S	SB	SB	SB	SB	SB	—	—		SB	
22B	S+S	SB	SB	SB	SB	SB	—	—		SB	
24A	S+S	SB	SB	AGN	SB	SB	SB	SB		SB	
24B	S+S	—	—	—	—	—	—	—	AGN	AGN	
26A	E+S	—	—	—	—	—	—	—		LL:	
26B	E+S	—	—	—	—	—	—	—	LLAGN	LLAGN	
27A	E+S	—	—	—	—	—	—	—	AGN	AGN	
27B	E+S	—	—	—	—	—	—	—	AGN	AGN	
28A	S+S	LINER	LINER	AGN	LINER	LINER	LINER	LINER		LINER	LINER
28B	S+S	SB	SB	SB	SB	SB	SB	SB		SB	
29A	S+S	SB	SB	SB	SB	SB	—	—		SB	
29B	S+S	SB	SB	SB	SB	SB	SB	SB		SB	
36A	S+S	—	—	—	—	—	—	—	AGN	AGN	
36B	S+S	—	—	—	—	—	—	—	AGN	AGN	
37A	S+S	—	—	—	—	—	—	—	AGN	AGN	NLAGN
37B	S+S	—	—	—	—	—	—	—	SB	SB	
39A	E+S	—	—	—	—	—	—	—	AGN	AGN	
39B	E+S	—	—	—	—	—	—	—		LL:	
44A	S+S	SB	SB	AGN	—	—	—	—		SB	
44B	S+S	—	—	—	—	—	—	—	AGN	AGN	
49A	E+S	—	—	—	—	—	—	—	SB	SB	
51B	E+E	—	—	—	—	—	—	—		LL:	
59A	S+S	—	—	—	—	—	—	—		LL:	
59B	S+S	—	—	—	—	—	—	—	AGN	AGN	
61A	E+S	—	—	—	—	—	—	—	AGN	AGN	
65A	E+S	SB	SB	SB	—	—	—	—		SB	
66A	S+S	SB	SB	AGN	SB	SB	—	—		SB	
68A	S+S	SB	SB	SB	SB	SB	SB	SB		SB	
68B	S+S	—	—	—	—	—	—	—	SB	SB	SB
69B	S+S	LINER	SB	AGN	LINER	SB	—	—		LINER	LLIRG
71A	S+S	—	—	—	—	—	—	—		LL:	
71B	S+S	—	—	—	—	—	—	—	AGN	AGN	
74A	S+S	SB	SB	SB	SB	SB	LINER	LINER		SB	
74B	S+S	SB	SB	SB	SB	SB	SB	SB		SB	
75A	E+S	—	—								

Table 6. Nuclear Activity classification

UZC-BGP	Pair type	Diag. 1			Diag. 2		Diag. 3		Diag. 4	Adopted	Known
		VO87	Kew01	Kauff03	VO87	Kew01	VO87	Kew01			
80B	S+S	–	–	–	–	–	–	–	SB	SB	
81A	S+S	SB	SB	SB/AGN	SB	SB	–	–		SB	
81B	S+S	SB	SB	AGN	SB	SB	SB	SB		SB	
82A	S+S	SB	SB	SB	SB	SB	–	–		SB	
83A	S+S	Sy 2	AGN	AGN	Sy 2	SB	Sy 2	Sy 2		Sy 2	Sy 2
83B	S+S	SB	SB	SB	SB	SB	SB	SB		SB	
84A	E+S	–	–	–	–	–	–	–		LL:	
84B	E+S	–	–	–	–	–	–	–	AGN	AGN	

classification into AGN, SB or LLAGN, according to diag. 4, is given. Column 7 reports the classification that we have adopted for each galaxy (LL: stands for LLAGN candidate, based on the unique presence of $[\text{NII}]_{6583}$ feature). Finally, column 8 reports the activity type classification available, for 11 galaxies, from NED.

Comparison of column 7 with column 8 shows a very good agreement between our classification and the available one. The agreement is very good also for the cases (UZC-BGP 2A, 5A and 83A) in which we have adopted the "majority" classification criterion and when the classification has been based only on H_α and $[\text{NII}]_{6583}$ (UZC-BGP 18A and 37A). Only for UZC-BGP 79A (NGC 6251) we could not confirm the Sy 2 nature as we did not detect H_β ³ (cfr. Table 3) at our imposed threshold limit for emission lines ($S/N \geq 5$).

From Table 6 we see that among the 65 galaxies with classified nuclear activity, 29 are SB, 18 AGN (including 2 LINERs and 1 Sy 2), 8 LLAGN and 10 LLAGN candidates. SB is the most common kind of nuclear activity encountered in our sample (30 % of galaxies display it), while AGN is limited to a smaller fraction (19 %) of galaxies. SBs are more commonly found in S+S pairs than AGNs. There are, in fact, 23/29 SB galaxies and 10/18 AGNs in S+S pairs (these last 10 include the 2 LINERs and the Sy 2), which implies a fraction of SB and AGN per spiral galaxy in S+S pairs of 50 % and 22 % respectively. The remaining 6 SBs are all hosted in the spiral member of E+S pairs, while the 8 AGNs equally divide between spirals and early-type galaxies, one (UZC-BGP 77A) of these last being actually hosted in a E+E pair. As a whole the fractions of SB and AGNs per spiral galaxy are 45 % and 22 % respectively. LLAGNs, instead, are exclusively found in E+S pairs and in half (4/8) cases this kind of activity is displayed by the early-type galaxy member of the pair. The distribution of LLAGN candidates (LL: in column 7 of Table 6) appears somewhat different from the LLAGN one, there are, in fact, 3/10 LL: in S+S pairs and of the remaining 7 LL: only 3 are

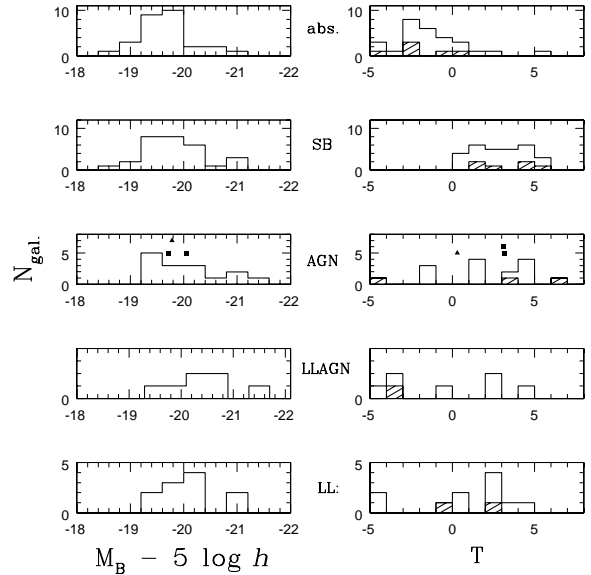


Fig. 8. Luminosity (M_B) and morphology (T) distribution of absorption line galaxies, SBs, AGNs, LLAGNs and LLAGN candidates. The dashed distributions in the right panels indicate morphological distribution of the brightest 20 % galaxies in each sample. In the AGN panels are indicated the position of the 2 LINERs (squares) and the Sy 2 (triangle) which have not been included in the histograms.

early-type galaxies. It is difficult to state whether the difference between LLAGNs and LLAGN candidates confirms previous finding (Ho et al. 1994) concerning the rather heterogeneous nature of LLAGNs, as our classification in LLAGN candidates has been based on the presence of the $[\text{NII}]_{6583}$ feature alone.

4. The relation between nuclear activity and host galaxy

Figure 8 shows the luminosity (M_B) and morphology (T) distribution of absorption line galaxies. SBs, AGNs, LLAGNs and LLAGN candidates. M_B has been derived from B_T which is available in LEDA for all but one LLAGN galaxy (UZC-BGP 10B). The dashed histogram in the morphological distribution (right panels) refer to the 20 % brightest galaxies in each sample. In AGN panels are also indicated magnitudes and types of

³ An extremely faint H_β emission, largely affected by an underlying strong absorption, is actually present in the spectrum of this galaxy, giving a $[\text{OIII}]_{5007}/H_\beta$ value of $3.20 (\pm 0.40)$. This last one, coupled to the $[\text{NII}]_{6583}/H_\alpha$ value of Table 5, would locate UZC-BGP 79A in the (VO87) Sy 2 region of diag. 1. However, since H_β feature is largely below our adopted threshold we maintain for this galaxy the AGN classification that we have derived on the basis of the $[\text{NII}]_{6583}$ and H_α features only (diag. 4).

the two LINERs (squares) and the Sy 2 (triangle) which have not been included in the histograms. Examining the left panels of Fig. 8 we see that galaxies displaying the largest B luminosity are LLAGNs, in fact most (71 %) of them have $M_B < -20 + 5 \log h$ a fraction which should be compared with 55 % of LLAGN candidates, 44 % of AGNs (LINERs and Sy 2 included), 35 % of SBs and 18 % of absorption line galaxies. These last ones are of particularly low B luminosity, quite unusual for passive galaxies which are, in general, much more luminous star forming ones (Kelm et al. 2005). Curiously, in our sample, absorption line galaxies and SBs have rather similar luminosity distribution which derive from an almost “opposite” morphological content. Further investigation is needed to understand if and how this population of low luminous early-type passive galaxies is connected to pair environment or if it is a more general characteristics of low density large scale environment.

The right panels of Fig. 8 show that absorption line galaxies are dominated by S0s ($-3 \leq T < 0$) and that very few of these galaxies display nuclear activity, ellipticals ($T < -3$), instead, show a much higher rate of nuclear activity and in some cases (AGNs and LLAGNs) are even among the 20 % brightest galaxies in each sample. Thus, low B luminosity coupled to absence of emission features seems to characterize more S0s than ellipticals, which, however, are much rarer than S0s in our sample.

The morphological distribution of SBs is rather flat and equally flat is the distribution of the brightest 6 among them. The first luminosity ranked ($M_B = -21.15 + 5 \log h$) SB is a late spiral (UZC-BGP 9B) and the second one ($M_B = -20.82 + 5 \log h$) UZC-BGP 2A, is an early spiral one. The median type of SB morphological distribution is 2.95 (corresponding to Sb) while, Ho et al. (1997) find a median value of 5 (corresponding to Sc) for their sample of galaxies with nuclear SB activity. Our sample is surely early spiral dominated but we could get, however, a larger median value of T if we had a larger content of late spirals among SBs. In our sample the fractions of early and late spiral SBs are extremely similar (19/44 and 9/20), while Ho et al. (1997) report fractions of 38 % and 82 %. However, if we separate 4-lines SBs (i.e. SB classified on the basis of at least 4 emission lines) from 2-lines SBs (classified based on H_α and $[NII]_{6583}$ features) we find both a B luminosity increase (63 % of these galaxies has $M_B < -20 + 5 \log h$) and a more advanced morphological type (median $T = 3.95$).

The morphological distribution of AGNs is rather advanced, the median value is 2.55 (\sim Sab) to be compared with 1 (\sim Sa) of Ho et al. (1997). AGNs are spread all over the morphological whole range and the 3 brightest AGNs reflect this behaviour too. The brightest ($M_B = -21.6 + 5 \log h$) AGN is UZC-BGP 79A an elliptical galaxy (NGC 6251) classified as Sy 2 (NED) showing, in our spectrum, an H_β emission well below our adopted S/N threshold, (see also sect. 3). The other two brightest galaxies have both $M_B < -20.7 + 5 \log h$ and advanced morphological type. The LINERs and the Sy 2, whose positions are represented with two squares and a triangle, display a modest luminosity. The morphological type of the LINERs is quite advanced too, for comparison Ho et al (1997) give a median value of 1.

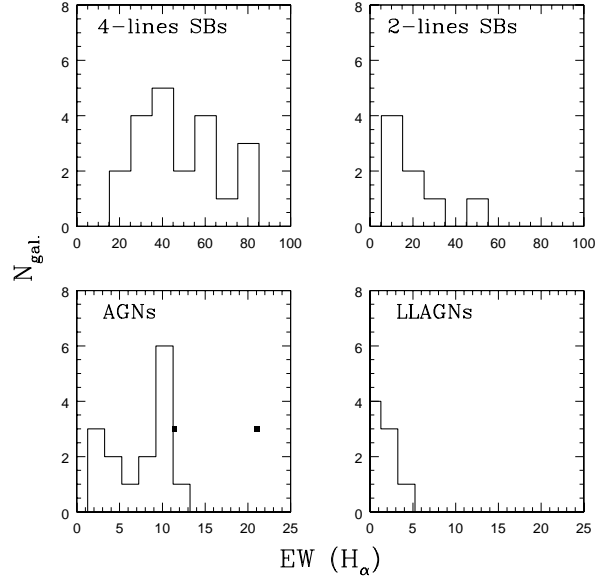


Fig. 9. H_α EW distribution of SBs classified on the basis of 4 (or more) emission lines (upper left) and of 2 emission lines (upper right), AGNs (lower left) and LLAGNs (lower right). The squares in the AGN panel indicate the position which would be occupied by the two LINERs (not included in the histogram). The Sy 2 position is not indicated as its H_α EW is the largest in the sample (117.43 Å) and would fall well behind the plot limits.

LLAGNs and LLAGN candidates distribute over the whole morphological range, their T morphological and luminosity distributions are somewhat different, LLAGN candidates displaying both a larger content of faint galaxies and spirals.

The EW of the H_α emission line of galaxies classified as SB (upper panels), AGN (lower left) and LLAGNs (lower right) is shown in Fig. 9. The upper left and right panels refer respectively to 4-lines SBs and 2-lines SBs. The squares in the AGN panel indicate the position which would be occupied by the two LINERs, not included in the histogram. The position of the Sy 2 is not marked as it would be too much far on the right in this plot, this galaxy has, in fact, the largest (117.43 Å) H_α EW of the whole sample.

The median values of the distribution of H_α EW of 4-lines SBs, 2-lines SBs, AGNs and LLAGNs are respectively 45.17 Å, 16.48 Å, 8.77 Å (9.67 Å including the Sy 2 and the LINERs) and 1.33 Å. For comparison Miller et al. (2003) report, for a large sample of SDSS galaxies having luminosity similar to ours but belonging to any kind of environments, median values of the H_α EW of 26 Å, 14 Å and 3 Å for 4-lines SBs, 2-lines SBs and AGNs respectively. Thus, while the 2-lines SBs display similar values of the median H_α EW, both 4-lines SBs and 2-lines AGNs show larger values in ours than in Miller et al. (2003) sample. However, the criterion adopted by Miller et al. (2003) to classify 2-lines AGNs is more conservative than the one adopted by us, as they required $\text{Log}([NII]/H_\alpha) > -0.2$. Application of their criterion to our data causes exclusion of 6 2-lines AGNs (belonging, obviously, to

the large values tail of H_α EW) and reduces the median value of 2-lines AGNs, in our sample, to 4.94 a value much more similar but still exceeding (1.6 times) the one reported by Miller et al. (2003). The excess, however, fades completely out if we include LLAGNs in our AGN sample as the median value of H_α EW drops to 2.34 Å, which is even below the value (3 Å) reported by Miller et al. (2003). The inclusion of LLAGNs, among AGNs, is justified since Miller et al. (2003) state that a significant population of their 2-lines AGNs are LLAGNs, although they do not say how many LLAGNs enter their AGN sample. Since LLAGNs are characterized by lower values of H_α EW than AGNs, the H_α EW of an AGN sample including also LLAGNs will reflect the relative amount of the two populations entering the sample. For this reason we do not expect exact coincidence between the value that we derive in our sample and the one reported by Miller et al. (2003) and we consider the agreement, between the two values, quite good. Thus only 4-lines SB in our sample display a median H_α EW which is significantly larger than the one reported by Miller et al. (2003) and which can not be attributed to instrumental effects as we find no correlation between the measured H_α EW and the S/N of the spectra.

In star forming galaxies the increase of H_α EW relates to the Star Formation Rate (SFR, Kennicutt & Kent 1983; Kennicutt et al. 1987). Thus the larger values displayed by 4-lines SB galaxies in our sample compared to the ones of Miller et al. (2003) supports the interaction - SB scenario. In this framework Barton et al. (2000) found a significant increase of H_α EW with decreasing galaxy-galaxy projected distance for SB galaxies in a magnitude limited sample of galaxy pairs. The correlation holds on a limited projected distance range (from $5h^{-1}$ to $40h^{-1}$ kpc) over which the H_α EW decreases from about 150 Å to 50 Å. Figure 9 shows that there are no SBs in our sample with H_α EW larger than 85 Å, that value is reached only by one galaxy (UZC-BGP 83B) whose projected distance from its companion (the only Sy 2 that we have detected in our sample) is $19h^{-1}$ kpc, which is small but not the smallest in the sample. The two SBs showing the smallest projected distance ($3h^{-1}$ kpc) in our sample belong to the same pair (UZC-BGP 74) and show H_α EW of 58.94 and 57.30 Å respectively. Half (15/29) of the SB in our sample display a value of H_α EW > 40 Å, which is supposed (Kennicutt & Kent 1984) to separate normal from intense SB activity. None of these intense-SB galaxies is found in pairs with a projected galaxy separation (r_p) larger than $160h^{-1}$ and 3 of them show $r_p < 30h^{-1}$. There are no other SBs with $r_p < 30h^{-1}$, while for $r_p > 160h^{-1}$ only 2 SBs are found (with an average value of H_α EW of 21.89 Å). We can not confirm the anticorrelation between H_α EW and galaxy-galaxy projected found by Barton et al. (2000), which is not surprising since our sample is quite different from theirs and we have few (9) galaxy pairs characterized by small ($\sim 50h^{-1}$ kpc) galaxy-galaxy separation. The lack of a clear anticorrelation in our sample might as well indicate that for bright isolated galaxies in pairs interaction is at work and effective up to $160h^{-1}$ kpc.

Figure 10 shows the M_H distribution of galaxies in our sample showing absorption lines (upper left) and classified as SB (upper right), AGN (lower left) and LLAGN/LLAGN candi-

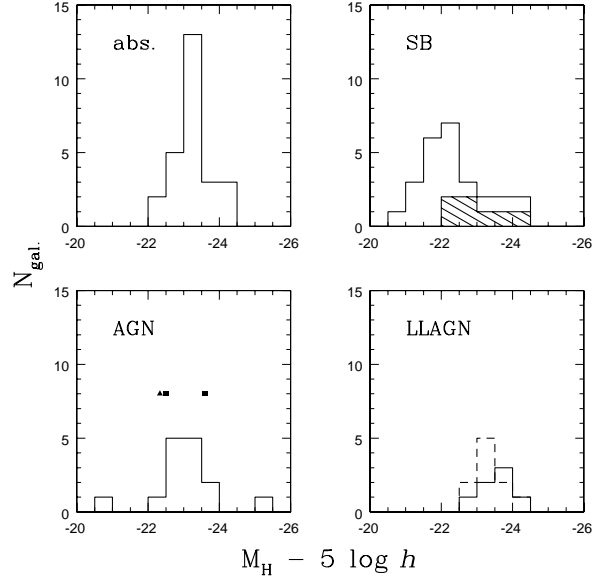


Fig. 10. M_H distribution of galaxies with absorption spectrum (upper left) and classified as SB (upper right), AGN (lower left) and LLAGN (lower right). The continuous distribution in the upper right panel represent the whole SB population, the dashed histogram 2-lines SBs. In analogy with Fig. 8 we have marked in the AGN panel (lower left) the position of the 2 LINERs (squares) and the Sy 2 (triangle) which have not been included in the histogram. In the lower right panel the continuous and dashed line refer respectively to LLAGNs and LLAGN candidates.

dates (lower right, continuous/dashed histogram). The continuous distribution in the upper right panel refers to the whole SB population, the dashed histogram to 2-lines SBs. M_H has been derived from 2MASS data available for all but 6 galaxies in our sample, which are 3 SBs (UZC-BGP 29B 49A and 74B), 2 absorption line galaxies (UZC-BGP 49B and 58B) and 1 LLAGN (UZC-BGP 26B). At variance with Fig. 8 in which galaxies display rather similarly large B luminosity distributions, Fig. 10 shows that only SBs have a broad M_H distribution extending over 4 magnitudes, in all the other cases galaxies are concentrated in a 2 magnitudes range. The only exception are AGNs whose distribution, however, appear large due to the presence of two galaxies only: the faintest and the brightest, in H, of the whole sample. The faintest ($M_H = -20.91 + 5 \log h$) is UZC-BGP 24B, an Sbc galaxy, the brightest ($M_H = -25.03 + 5 \log h$) is UZC-BGP 79A an elliptical, whose Sy 2 nature we do not confirm due to our imposed emission line S/N threshold. From Fig. 10 we see that while 10/26 SB galaxies have $M_H \geq -22 + 5 \log h$, there are no absorption line galaxies fainter than that limit and only 1/18 AGNs. LLAGNs and LLAGN candidates are even brighter as they all show $M_H < -22.5 + 5 \log h$. The upper right panel of Fig. 10 shows that 2-lines SBs (dashed histogram) are all found at large H luminosity and constitute more than half of the whole “H luminous” ($M_H > -22.5 + 5 \log h$) SB population. A KS test confirms (99.3 c.l.) the difference between 4-lines SB and 2-lines SB M_H distribution. The M_H distribution of SBs, as a whole, differs significantly from the

one of absorption line galaxies, AGNs, LLAGNs and LLAGN candidates (KS c.l. $>> 99.9\%$, 99.7% , 99.1% and 99.9% respectively). The significance of these differences becomes, obviously, larger if we exclude from SB class the 2-lines SBs, (in this case we obtain a KS c.l. always $> 99.9\%$ for 4-lines SB vs. AGN, LLAGN and LLAGN candidates respectively).

The luminosity in H relates to the galaxy mass within the optical radius of disc galaxies (M_{dyn}) a quantity which can be derived through the relationship $\log(M_{dyn}/M_{\odot}) = \log(L_H/L_{H\odot}) + 0.66$ (Gavazzi et al. 1996). Adopting M_H sun = 3.39 (Allen 1973) we have calculated M_{dyn} for all the disc galaxies (i.e. elliptical excluded) in the sample having H magnitude available. The results are summarized in Table 7 where we indicate for each activity type (column 1), the total number of galaxies (N_T) (column 2), the number of galaxies (N_H) having H magnitude available (column 3) and the number of galaxies ($N_{M_{dyn}}$) for which we have derived the galaxy mass (M_{dyn}), (column 4). In column 5 we give the minimum and maximum value of the mass for each distribution (ΔM_{dyn}) and in column 5 the median value of each distribution ($med(M_{dyn})$). With the term none (first row of column 1) we indicate galaxies with absorption lines only in their spectrum. Since the nature of S0 galaxies is somewhat questioned and since among them there might be some misclassified ellipticals we have also computed M_{dyn} for spiral galaxies only. The results, only if different from values reported in columns 3, 4 and 5, are shown in columns 6, 7 and 8 in which we indicate number of spiral galaxies ($N_{spir.}$), minimum and maximum value of the mass ($\Delta M_{spir.}$) and median value of the mass distribution ($med(M_{spir.})$). The exclusion of S0s does not change significantly the results as mass ranges remain the same, in all but the sample of absorption line galaxies, and median values display, consequently, modest changes (only for LLAGNs and LLAGN candidates).

Absorption line galaxies, LLAGNs and LLAGN candidates display the higher value of the mass, SB the lowest as this is the only population with a median value of the mass distribution below $10^{11} M_{\odot}$. However if we separate 2-lines SBs from 4-lines SBs the median value of the first ones increases to $1.3 \cdot 10^{11} M_{\odot}$ and the mass range narrows (between $7.8 \cdot 10^{10}$ and $4.4 \cdot 10^{11} M_{\odot}$), while the second ones display a mass range between $2.5 \cdot 10^{10}$ and $4.5 \cdot 10^{11} M_{\odot}$ and median value of $6.5 \cdot 10^{10} M_{\odot}$. AGNs appear characterized by a wide mass distribution too, which is induced by the presence of an extremely low mass galaxy (UZC-BGP 24B, see also Fig. 10 and relative comments). Exclusion of this galaxy from the AGN sample would raise the minimum mass to $7.9 \cdot 10^{10}$ (still below the minimum for absorption line galaxies, LLAGNs and LLAGN candidates) and the median value to $1.6 \cdot 10^{11} M_{\odot}$.

Kauffmann et al. (2003) have shown that AGNs reside only in galaxies with masses $M > 10^{10} M_{\odot}$, a value that should be scaled to $0.7 \cdot 10^{10} M_{\odot}$ to account for the different value of H_0 adopted by us and by them. Table 7 shows that, due to the imposed criterion on luminosity (see also sect. 2), all galaxies in our sample have masses above the Kauffmann et al. (2003) value, we are thus unable to confirm their finding.

Figure 11 illustrates the Color Magnitude (CM) diagram (B-H vs. M_H) for galaxies with absorption spectra (upper left) and classified as SB (upper right), AGN (lower left), LLAGN

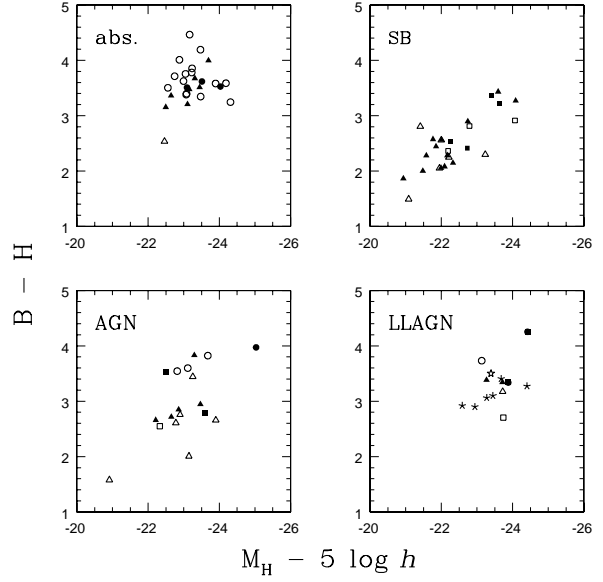


Fig. 11. Color magnitude diagram (B-H vs. M_H) for galaxies with absorption spectra (upper left) and classified as SBs (upper right), AGNs (lower left), LLAGNs and LLAGN candidates (lower right). Filled and empty circles and triangles indicate, in each panel ellipticals, S0s, early and late spirals. In the SB panel (upper right) the previously defined symbols indicate morphological classification of 4-lines SBs, while filled and empty squares indicate early and late spirals of 2-lines SBs. In the AGN panel (lower left) filled and empty squares indicate, instead, the 3 galaxies classified respectively as LINERs and Sy 2. In the LLAGNs/LLAGN candidates panel (lower right) the standard symbols (filled/open circles/triangles) have been used to distinguish LLAGN morphological types while we have used filled/open squares to indicate LLAGN candidates ellipticals and S0s and filled/empty stars to indicate early/late spirals.

and LLAGN candidates (lower right). We distinguish, for each activity class, different morphological types. As a general rule filled and empty circles indicate ellipticals and S0s, while filled and empty triangles stand for early and late spirals. This rule holds for the absorption line galaxies, 4-lines SBs (although this class of objects does not contain early-type galaxies), AGNs and LLAGNs. Concerning 2-lines SBs (upper right panel) early and late spirals are indicated as filled and empty squares, while for LLAGN candidates (lower right panel) we have adopted filled and empty squares to indicate E and S0s and filled and empty stars to indicate early and late spirals. Finally in the AGN panel (lower left) empty and filled squares indicate the Sy 2 and LINERs location respectively (all three are early spirals).

Absorption line galaxies (upper left panel of Fig. 11) occupy a well defined “red-bright” region in the CM diagram, with the exception of UZC-BGP 8A (NGC 800) which is the only late type spiral, with an absorption spectrum, in our sample. The absence of a trend for absorption line galaxies in the CM diagram must be attributed to the large group of S0s

Table 7. The mass of galaxies with different nuclear activity type

Activity	N_T	N_H	$N_{M_{dyn}}$	ΔM_{dyn} ($10^{11} M_\odot$)	Med (M_{dyn}) ($10^{11} M_\odot$)	$N_{spir.}$	$\Delta M_{spir.}$ ($10^{11} M_\odot$)	Med ($M_{spir.}$) ($10^{11} M_\odot$)
none	28	26	23	[1.0 : 5.5]	1.9	8	[1.0 : 3.1]	
SB	29	26	26	[0.3 : 4.5]	0.8			
AGN	18	18	17	[0.2 : 3.8]	1.5	15		
LLAGN	8	7	5	[1.2 : 3.2]	2.1	4		2.6
LL:	10	10	8	[1.1 : 6.0]	2.4	7		2.2

(empty circles) which dominate this population. In fact early spirals with an absorption spectrum (filled triangles) follow the expected trend and get more H luminous as they become redder (B-H increasing). SB galaxies (upper right panel) follow a much better defined sequence which holds on a wide range of luminosities. The large proportion of filled vs. empty symbols indicate the dominance of early spirals among this class of objects. The faint luminosity region is mostly occupied by a population of early spirals which besides being quite faint ($M_H \leq -22 + 5 \log h$) are also exceptionally “blue” (B-H ~ 2.2). As expected (cfr. Fig. 9) early and late spirals classified as 2-lines SBs (filled and empty squares) occupy the high H luminosity “red” region of the diagram. They too follow the general SB trend. The AGN panel shows the absence of a trend and all but 2 (the brightest and the faintest) AGNs are concentrated in a narrow region which resembles the absorption line galaxies “cloud” but which is characterized by a bluer color and a somewhat fainter H luminosity. The AGN “cloud” is actually made of two different regions which are characterized by similar H luminosity and different color. The separation of the two AGN regions occurs at B-H ~ 3 , which is also the value below which almost no absorption line galaxies are found and where most SB galaxies reside. Also LLAGN and all but one LLAGN candidates occupy a well defined region in the CM diagram which is brighter than the ones occupied by absorption line galaxies and AGNs and has the color in between the two. As a whole Fig. 11 indicates that absorption line galaxies, SBs, AGNs and LLAGNs occupy rather distinct regions in this CM diagram so that it would be possible to distinguish SB from absorption line galaxies only on the basis of their location in this diagram. AGN location is in between the previous two, but almost completely separated from the one of LLAGN and LLAGN candidates. This is an interesting finding that should be checked on galaxy samples in different environments.

5. Nuclear activity in pairs showing evident interaction

There are cases in which galaxy interaction produces “visible” effects such as morphological distortions, bridges and tidal tails. The detection of those features depends, however, on the sensitivity to low surface brightness structures and is thus strongly affected by seeing, depth and redshift. Moreover morphological distortions are short living phenomena (100 Myr) and tidal tails appear only in prograde disk encounters (Toomre & Toomre 1972). Thus a selection of systems based on the presence of “visible” signs of interaction would surely lead to miss

a fraction of interacting pairs. However, pairs showing evident interaction can be used to test the pair sample as a whole, as differences that might be present in the content and type of nuclear activity between these systems and the whole pair sample could bring into question the interaction status of galaxy pairs.

Careful inspection of DSS images of all pairs in our sample allowed us to identify 9 pairs in which interaction is clearly “visible” between the members. These pairs are listed in Table 8, where we give, for each of them, identifier (column 1), pair/galaxy morphology (column 2; as in Tables 4, 5 and 6 galaxy morphology of the active member is underlined in case of E+S pair), nuclear activity type (column 3; – indicate absence of nuclear activity) and H_α EW (column 4; only if the galaxy is active).

Among the 48 galaxy pairs which constitute our sample only 9 (listed in Table 8) are characterized by evident signs of interaction between their members. Table 8 shows that this happens more frequently in S+S (6/23) than in E+S (3/19) pairs and that in these last cases interaction is never able to induce emission activity in the early type member of the pair. On the other hand evident interaction does not appear to be able to induce nuclear activity in 2 galaxies belonging to the S+S pairs either. All kinds of activities are found in pairs listed in Table 7; visible interaction thus does not appear to be responsible for activation of a particular kind of nuclear activity. In Table 8 there are 7 SB galaxies, 3 AGNs (Sy 2 included), 1 LLAGN, 2 LLAGN candidates and 5 galaxies with absorption spectrum. This implies fractions of activity type per galaxy of 39 %, 17 %, 6 %, 11 % and 28 % which are remarkably similar to the ones holding for the whole sample (30 %, 19 %, 8 %, 11 % and 30 %). Five of the SBs in Table 8 are 4-lines SBs, two (UZC-BGP 8A and 49A) are 2-lines SBs. Thus also the fraction of 2 over 4-lines SBs in these pairs agrees remarkably well with the fraction in the whole sample (8/21). From column 5 of Table 8 we can derive the median value of H_α EW of 4-lines and 2-lines SB respectively 58.94 Å and 16.49 Å, again very similar to the ones derived for the whole sample (cfr. sect. 4). The similarity in terms of amount, type and characteristics of the nuclear activity content between these 9 pairs and the whole sample supports the hypothesis that galaxy-galaxy interaction between bright galaxies in isolated pairs is at work and effective.

Since UZC-BGP is a volume-limited sample, evident interaction may even occur between one pair member and a faint companion which has gone undetected either by UZC catalog magnitude limit ($m_{Zw} \leq 15.5$) or by UZC-BGP luminosity limit ($M_{Zw} \leq -18.9 + 5 \log h$). This happens for 9 galaxies, belonging

Table 8. UZC-BGPs showing interaction between members

UZC-BGP	Pair type	Activity type		H_α EW	
		A	B	A	B
8	S+S	–	SB	–	12.46
14	E+S	SB	–	74.51	–
21	E+S	–	LLAGN	–	0.31
49	S+S	SB	–	20.51	–
59	S+S	LL:	AGN	–	9.39
65	E+S	SB	–	43.47	–
71	S+S	LL:	AGN	–	1.84
74	S+S	SB	SB	58.94	57.30
83	S+S	Sy2	SB	117.43	85.01

Table 9. UZC-BGP galaxies interacting with fainter companions

UZC-BGP	Pair type	Activity type	H_α EW	Companion
4B	E+S	LLAGN	0.34	IC 1559
5B	E+S	–	–	NGC 197
9B	S+S	SB	11.22	NGC 876
10A	E+S	LLAGN	1.66	NGC 997N
16A	E+S	–	–	NGC 1588
20A	E+S	SB	76.86	NGC 2744S
20B	E+S	LLAGN	1.02	NGC 2751
26B	E+S	LLAGN	0.47	IC 590 E
28A	S+S	LINER	11.42	NGC 3303 N

Table 10. UZC-BGPs with absorption line spectrum in both members

UZC-BGP	Pair type	Interaction
23	E+E	A with NGC 2988
31	S+S	no
35	E+E	A with B
58	E+E	A with B
63	E+E	no
67	E+S	no
76	S+S	no

to 8 distinct pairs, which we list in Table 9. For each galaxy we give identifier (column 1), pair/galaxy morphology (column 2; as in Table 8 galaxy morphology is underlined in case of E+S), activity type (column 3; as in Table 8 – means no activity), H_α EW, identifier of the companion (column 5). Among these faint companions only two (NGC 1588 and NGC 2751) interacting respectively with UZC-BGP 16A and 20B have failed the luminosity limit of UZC-BGP, in all other 7 cases companions were too faint to be included in the UZC catalog.

At variance with Table 8, Table 9 shows that most (7/9) of the galaxies interacting with fainter companions belong to E+S pairs. Five galaxies in Table 9 are early-type, two of them (UZC-BGP 5B and 16A) display no activity while the remaining three (UZC-BGP 10A, 20B and 26B) show LLAGN activity. This last one is the most frequent kind of activity of galaxies in Table 9. The fraction of LLAGNs among the galaxies of Table 9 is 44 % (to be compared with 8 % on the whole sample). The excess of LLAGNs could indicate minor galaxy

interaction (Woods & Geller 2007) as a driving mechanism for this kind of activity. Interestingly the interacting LLAGNs of Table 9 are all found in E+S pairs which we expected (cfr. Fig.3 and discussion) to be possibly, in large part, the bright core of a looser structure. The presence of a fainter close companion confirms both our expectation and previous finding (Coziol et al 1998, 2000; Martinez et al. 2006) which claim LLAGN to be the most common kind of activity in Compact Groups. Further investigation is needed since no detailed analysis concerning the link between LLAGN activity and interaction has been carried out so far.

Finally, if interaction plays a major role in activating nuclear activity passive galaxies in galaxy pairs should not display evident interaction signs. There are 7 pairs in our sample with both members passive. They are listed in Table 10 where we give, pair identifier (column 1), morphology (column 2) and, in column 3, we indicate if interaction occurs between pair members or with a faint companion. Only one galaxy (UZC-

BGP 23A) interacts with a faint companion (NGC 2988 which was not included in UZC catalog). The sample is dominated by (4/7) by E+E pairs, 3 of which show interaction patterns, the remaining 2 S+S and E+S pairs do not show interaction at all. There is evident interaction and no activity only in the 3 E+E pairs, which is somewhat encouraging for the interaction-activity scenario as galaxy interaction is surely going to produce larger effects in gas rich than in gas poor galaxies, while the 2 S+S pairs are characterized by large values (159 and $183 h^{-1}$ kpc) of r_p (cfr. Fig. 3, upper middle panel) in our sample. This confirms our previous finding on H_α EW and suggest that in UZC-BGP sample interaction is at work and effective up to $160 h^{-1}$ kpc.

6. Conclusions

To investigate the role of galaxy interaction on nuclear activity we have performed a detailed spectroscopical analysis on 48 galaxy pairs, which represent more than half of the whole UZC-BGP sample and have an excellent morphological match with it.

We have found an extremely large fraction of emission line galaxies in our sample particularly among early (84 %) and late (95 %) spirals.

Classification and analysis of spectral activity, performed by means of standard diagnostic diagrams, allowed us to show that SB is the most frequent (30 % of galaxies) kind of activity in our sample. It occurs exclusively in spiral galaxies with a frequency of SB phenomenon among spirals of 45 %. The blue luminosity distribution of these SB is not particularly high as 67 % have $M_B > -20 + 5\log h$.

While SB are preferentially found in S+S pairs, AGN are almost equally found in S+S and in E+S pairs although in most cases (82%) this kind of activity is displayed by a spiral galaxy. AGN in our sample show, in fact, a rather advanced morphological distribution characterized by a high blue luminosity. The fraction of AGNs in late spirals is 35 % and late spirals hosting AGNs have an average $M_B = -20.4 + 5\log h$.

SBs display enhanced H_α EW an effect which relates to star formation and might thus be related to pair environment. Star formation turns out to be intense in half of the SB galaxies in our sample. Intense-SBs have galaxy-galaxy separations up to $160 h^{-1}$ kpc implying that interaction may be effective in isolated pairs of bright galaxies up to that distance.

Absorption line galaxies, SBs, AGNs and LLAGNs (candidates included) occupy rather distinct locations in the B-H vs M_H diagram a characteristics which reflects the different distribution in B and H luminosity of each sample. Galaxy masses, estimated using the H luminosity, are high for absorption line galaxies and LLAGNs (as a whole), low for SBs and "intermediate" for AGNs

All LLAGNs reside in E+S and are equally distributed between early type galaxies and spirals. We have shown that half of them are hosted in galaxies displaying visible signs of interaction with fainter companions, which suggests that minor interaction might be a driving mechanism from a relevant fraction of LLAGNs. LLAGN has been claimed to be a heterogeneous class of objects: our previous finding concerning only half

of the whole LLAGN population, coupled with the quite different behaviour in terms of blue luminosity and morphological content of LLAGN candidates appear to confirm that claim.

Acknowledgements. This work was supported by MIUR. P.F acknowledges financial support from the contract ASI-INAF I/023/05/0. S.M. acknowledges a fellowship by INAF-OAB. This research has made use of the NASA/IPAC Extragalactic Database (NED) and of the Hyperleda Database (<http://leda.univ-lyon1.fr/>). We thank an anonymous referee whose comments and criticism greatly improved the scientific content of the paper.

References

- Allen, C. 1973, *Astrophysical Quantities*, The Athlone Press (London)
- Alonso, M.S., Tissera, P.B., Colwell, G., & Lambas, D. 2004, *MNRAS*, 352, 1081
- Bahcall, N.A., Lubin, J.M., & Dorman V. 1995, *ApJ*, 447, L81
- Baldwin, J. A., Phillips, M. M., & Terlevich, R. 1981, *PASP*, 93, 5
- Barnes J.E., & Hernquist L.E. 1991, *ApJ*, 370, 65
- Barton, E.J., Geller M.J., & Kenyon S.J. 2000, *ApJ*, 530, 660
- Borne, K.D., Bushouse, H., Colina, L., et al., 1999, *Ap & SS*, 266, 137
- Bundy, K., Fukugita, M., Ellis, R.S., Kodama, T., Conselice, C.J., 2000, *ApJ*, 601, 123
- Carlberg, R.G., Pritchet, C.J., & Infante, L., 1994 *ApJ* 435, 540
- Coziol, R., Ribeiro, A.L.B., de Carvalho, R.R., & Capelato, H.V. 1998, *ApJ*, 493, 563
- Cid Fernandes, R., Gonzales D., Rosa M., et al. 2004, *ApJ* 605, 105
- Cuesta-Bolao, M.J., & Serna, A. 2003, *A&A*, 405, 917
- Dahari, O. 1985, *ApJS*, 57, 643
- De Robertis, M.M., Hayhoe, K., & Yee, H.K.C. 1998, *ApJS*, 115, 163
- Donzelli, C. & Pastoriza, M.G. 1997, *ApJS*, 111, 181
- Dubinski, J., Mihos, J.C., & Hernquist, L., 1996, *ApJ* 462, 576
- Falco, E.E., Kurtz, M.J., Geller, M.J., et al. 1999, *PASP*, 111, 438
- Focardi, P., & Kelm, B. 2002, *A&A*, 391, 35
- Focardi, P., Zitelli, V., Marinoni, S., & Kelm, B. 2006, *A&A*, 456, 467 (paper I)
- Fuentes-Williams, T., & Stocke, J.T. 1988, *AJ*, 96, 1235
- Gavazzi, G., Pierini, D., & Boselli, A. 1996, *A&A*, 312, 397
- Gonçalves, A. C., Véron-Cetty, M.-P., & Véron, P. 1999 *A&AS*, 135, 437
- Gottlober, S., Klypin, A., & Kravstov, A.V., 2001, *ApJ* 546, 223
- Governato, F., Gardner, J.P., Stadel, J., Quinn, T., & Lake, G., 1999, *MNRAS* 307, 949
- Ho, L.C., Filippenko, A.V., & Sargent, W.L.W., 1994, *IAU Symp.*, 159, 275
- Ho, L.C., Filippenko, A.V., & Sargent, W.L.W. 1997, *ApJ*, 487, 568
- Karachentsev, I.D. 1972, in *Catalogue of Isolated Pairs in the Northern Hemisphere, Comm. Spec. Ap. Obs.*, 7, 1 (KPG)
- Kauffmann, G., Heckman, T.M., Tremonti, C., et al. 2003, *MNRAS*, 346, 1055
- Keel, W.C., Kennicutt, R., Hummel, E., & van der Hulst, J. 1985, *AJ*, 90, 708
- Keel, W.C. 1993, *AJ*, 106, 1771
- Keel, W.C. 1996, *AJ*, 111, 696
- Kelm, B., Focardi, P., & Palumbo, G.G.C. 1998, *A&A*, 335, 912
- Kelm, B., Focardi, P., & Zitelli V. 2004, *A&A*, 418, 25
- Kelm, B., & Focardi, P. 2004, *A&A*, 418, 937
- Kelm, B., & Focardi, P., & Sorrentino, G., 2005, *A&A*, 442, 117
- Kennicutt, R.C.Jr., & Kent, S.M., 1983, *AJ*, 88, 1094
- Kennicutt, R.C.Jr., & Keel, W.C. 1984, *ApJ*, 279, L5
- Kennicutt, R.C.Jr., Kennicutt, R.C.Jr., Keel, W.C., van der Hulst, J.M., Hummel, E., 1987, *AJ*, 93, 1011

- Kennicutt, R.C.Jr., Tamblin, P., & Congdon, C.E. 1994, *ApJ*, 435, 22
- Kewley, L., Dopita, M., Sutherland, R., Heisler, C., Trevena, J. 2001, *ApJ*, 556, 121
- Kewley, L.J., Groves, B., Kauffmann, G., & Heckman, T. 2006, *MNRAS*, 372, 961
- Larson, R.B., & Tinsley, B.M. 1978, *ApJ*, 219, 46L
- Lauberts, A., & Valentijn, E. 1989, *The Surface Photometry Catalogue of the ESO-Uppsala Galaxies*, ESO, Garching bei Munchen (ESO-LV)
- Le Fevre, O., Abraham, R., Lilly, S., 2000, *MNRAS*, 311, 565
- MacKenty, J.W. 1989, *ApJ*, 343, 125
- Martinez, M.A., del Olmo, A., Perea, J., & Coziol, R. 2006, in *Groups of Galaxies in the Nearby Universe*, ESO-workshop, [astro-ph/0611098]
- Mihos, J., & Hernquist, L., 1996, *ApJ* 464, 641
- Miller, C.J., Nichol, R.C., Gomez, P.L., Hopkins, A.M., & Bernardi, M. 2003, *ApJ*, 597, 142
- Noguchi, M. 1988, *A&A*, 203, 259
- Patton, D.R., Carlberg, R.G., Marzke, R.O., et al., 2000, *ApJ* 536, 153
- Paturel, G., Petit, C., Prugniel, Ph., et al. 2003, *A&A* 412, 45
- Rafanelli, P., Violato, M., & Baruffolo, A. 1995, *AJ*, 109, 1546
- Reduzzi, L., & Rampazzo, R. 1995, *ApJL & Comm.*, 30, 1 (RR)
- Sanders, D.B., & Mirabel, I.F. 1996, *ARA&A*, 34, 749
- Sanders, D.B., Soifer, B.T., Elias, J.H., et al. 1988, *ApJ*, 325, 74
- Schmitt, H.R. 2001, *AJ*, 122, 2243
- Toomre, A., & Toomre, J. 1972, *ApJ*, 178, 623
- Veilleux, S., & Osterbrock, D. E. 1987, *ApJS*, 63, 295
- Veilleux, S., Kim, D.C., Sanders, D.B., Mazzarella, J.M., & Soifer, B.T. 1995, *ApJS*, 98, 171
- Veilleux, S. 2002, in *AGN Surveys*, ed. R.F. Green, E.Ye. Khachikian, & D.B. Sanders, IAU Coll. 184, ASP Conf. Proceed. 284, 111
- Véron, P., Gonçalves, A.C., & Véron-Cetty, M.P. 1997 *A&A*, 319, 52
- Woods, D. F., & Geller, M. 2007, *AJ* 134, 527
- Zepf, S.E., & Koo, D.C., 1989, *ApJ* 337, 34